

## Sensors and Actuators: B. Chemical

### A benzimidazole-based new fluorogenic differential/sequential chemosensor for Cu<sup>2+</sup>, Zn<sup>2+</sup>, CN<sup>-</sup>, P<sub>2</sub>O<sub>7</sub><sup>4-</sup>, DNA, its live-cell imaging and pyrosequencing applications --Manuscript Draft--

<b>Manuscript Number:</b>	
<b>Article Type:</b>	Research Paper
<b>Section/Category:</b>	Optical Sensors
<b>Keywords:</b>	Benzimidazole, Differential Cu <sup>2+</sup> and Zn <sup>2+</sup> sensor, Cyanide and PPI-sensor, Metastatic cells, Metal-based DNA-sensor, PPI-detection in PCR products.
<b>Corresponding Author:</b>	Anbu Sellamuthu, Ph.D University of Hull Birmingham, UNITED KINGDOM
<b>First Author:</b>	Anbu Sellamuthu, Ph.D
<b>Order of Authors:</b>	Anbu Sellamuthu, Ph.D Anup Paul, PhD Kalpana Surendranath, PhD Nadeen Shaikh Solaiman Armando J. L. Pombeiro
<b>Abstract:</b>	<p>Differential chemosensors have emerged as next-generation systems due to their simplicity and favourable responsive properties to produce different signals upon selective binding of various analytes simultaneously. Nevertheless, given their inadequate fluorescence response and laborious synthetic procedures, only a few differential chemosensors have been developed so far. In this work, we have employed a single-pot synthesis strategy to establish a new benzimidazole-based fluorogenic chemosensor (DFB) which differentially detects Cu<sup>2+</sup> (detection limit (LOD) = 24.4 ± 0.5 nM) and Zn<sup>2+</sup> (LOD = 2.18 ± 0.1 nM) through fluorescence “off-on” manner over the library of other metal cations in an aqueous medium. The DFB-derived ‘in situ’ complexes DFB-Cu<sup>2+</sup> and DFB-Zn<sup>2+</sup> showed fluorescence revival “on-off” responses toward cyanide (CN<sup>-</sup>) and bio-relevant pyrophosphate (P<sub>2</sub>O<sub>7</sub><sup>4-</sup>--PPI) ions with a significantly low LOD of 9.43 ± 0.2 and 2.9 ± 0.1 nM, respectively, in water. We have demonstrated the phosphate group-specific binding capability of DFB-Zn<sup>2+</sup>, by testing it with both ssDNA and dsDNA samples which displayed fluorescence “turn-off” response (LOD 10<sup>-7</sup> M), similar to the PPI binding in an aqueous medium, indicating that it interacts explicitly with the phosphate backbone of DNA. We have also harnessed the DFB as a sequential fluorescent probe to detect Cu<sup>2+</sup>, Zn<sup>2+</sup>, CN<sup>-</sup> and P<sub>2</sub>O<sub>7</sub><sup>4-</sup> ions in human cervical (HeLa) and breast (MCF-7 and MDA-MB-231 (aggressive and invasive)) cancer cell lines. Moreover, we have explored the PPI recognition capability of DFB-Zn<sup>2+</sup> in the polymerase-chain-reaction (PCR) products where PPI is one of the primary by-products during amplification of DNA.</p>
<b>Suggested Reviewers:</b>	<p>Shiguo Sun Northwest A&amp;F University: Northwest Agriculture and Forestry University gsnus@fauswn.ude.cn Dr Sun is one of the renowned research leaders in the field of supramolecular chemistry.</p> <p>Thenmozhi Kathavarayan Vellore Institute of Technology: VIT University kt.thenmozhi@gmail.com Dr Thenmozhi is researching in the development of sensor systems for the detection of bio-relevant molecules.</p> <p>Cheal Kim Seoul National University of Science and Technology chealkim@seoultech.ac.kr Dr Cheal Kim's research group is involving in the development of Schiff base type Chemosensors for metal ions.</p>

Viswanathamurthi Periasamy  
Professor, Periyar University  
viswanathamurthi72@gmail.com  
Prof. Viswanathamurthi is one of the research leaders in the field of coordination chemistry and biological chemistry.

Andrew G. Sykes  
University of South Dakota  
asykes@usd.edu  
Dr Andrew G. Sykes researching in the field of fluorescent sensors and Inorganic chemistry.

Dear Editor,

Thank you for your comments on our previously submitted version of the manuscript (SNB-D-20-05236). As per your comments and suggestions, we have thoroughly reformulated the manuscript and included the data (wherever applicable).

We would like to resubmit for your consideration the ‘reformulated’ manuscript entitled “*A benzimidazole-based new fluorogenic differential/sequential chemosensor for Cu<sup>2+</sup>, Zn<sup>2+</sup>, CN<sup>-</sup>, P<sub>2</sub>O<sub>7</sub><sup>4-</sup>, DNA, its live-cell imaging and pyrosequencing applications*” for publication as a full paper.

**Comment 1:** No detailed comparison with the performance of known sensors/probes (mostly optical) for the determination of the various analytes (ions, DNA) is provided. For instance, insert Tables in the Suppl. Information and discuss them in the main text.

**Response:** We have now showcased 12 literature reported sequential chemosensor systems in a Table (S1, Supplementary Information) with the following details that include signalling/fluorophore units, analyte receptor units, the medium of access, sensing capability in terms of analyte binding constant and detection limit values and method, mode and mechanism. Also, we have compared with several ‘turn-on’ Cu<sup>2+</sup>-sensors in appropriate places and introduced a new section (Comparison of sequential sensing performance) in the main text and compared with our sequential sensor system (**DFB**) in detail.

**Comment 2:** - While the spectroscopic characterization of the probe-metal interaction is thorough, the analytical characterization is far from complete (as per SNB Aims & Scope). Uncertainty values must be shown in calibration plots and other relevant datasets to allow proper calculation of the limit of detection and other features (the linearity of the dose-response curves at low analyte concentrations is poor). Parameters such as limit of detection, dynamic range, interferences, repeatability, reproducibility, etc. (where applicable) have not been determined for some species.

**Response:** We appreciate the Editor for these valuable suggestions. Accordingly, we have now synthesized the chemosensor (**DFB**) derived Cu(II) and Zn(II) complexes (**DFB-Cu<sup>2+</sup>** and **DFB-Zn<sup>2+</sup>**) and fully characterized them by both analytical and spectroscopic methods (please see the experimental section in the main text) including elemental analyses, IR and HRMS techniques

(Figs. S4 and S5). Also, the binding constants and limiting of detection (LOD) values of the sensor compounds were also recalculated and included in the text with standard deviation (errors) and discussed.

**Comment-3:** - The sensor has not been applied to the analysis of relevant real samples (e.g. plasma, waters). This is a key issue for SNB manuscripts (see <https://www.journals.elsevier.com/sensors-and-actuators-bchemical>). Therefore, its value cannot be assessed.

**Response:** We are grateful to the Editor for this valuable comment. Accordingly, we have harnessed the sensor **DFB** as a sequential fluorescent probe to detect  $\text{Cu}^{2+}$ ,  $\text{Zn}^{2+}$  and  $\text{P}_2\text{O}_7^{4-}$  ions in human cervical (HeLa) and breast (MCF7 and MDA-MB 231 (metastatic)) cancer cells. Moreover, we have explored the PPI recognition capability of **DFB-Zn<sup>2+</sup>** in the polymerase-chain reaction (PCR) product mixture where PPI is one of the major by-products during amplification of DNA. These critical application sections are also included in the current version of Manuscript and Supplementary Information.

Considering these results altogether, we believe that the current version of this manuscript meets the standard of “Sensors and Actuators: B Chemical” journal. We also believe that the work is interdisciplinary, within topics of current interest in Inorganic, Analytical Chemistry and Biology, Genetics, and we think it fulfils the conditions to be considered for publication in “Sensors and Actuators: B Chemical” journal.

We thank you for your kind consideration.

Sincerely,

Sellamuthu Anbu

Anup Paul

Kalpana Surendranath

Nadeen Sheikh Solaiman

Armando J. L. Pombeiro

## Research Highlights

- A benzimidazole-based chemosensor (**DFB**) shows “*off-on*” responses upon differential detection of  $\text{Cu}^{2+}$  (LOD = 24 nM) and  $\text{Zn}^{2+}$  (LOD = 2.18  $\mu\text{M}$ ).
- The **DFB** derived  $\text{Cu}^{2+}$ , and  $\text{Zn}^{2+}$  complexes serve as efficient secondary sensors toward  $\text{CN}^-$ , PPI and DNA in an aqueous medium.
- **DFB** acts as a sequential fluorescent probe to detect  $\text{Cu}^{2+}$ ,  $\text{Zn}^{2+}$  and PPI in living cancer cells.
- **DFB-Zn<sup>2+</sup>** can detect the PPI in the PCR amplified DNA products.

**A benzimidazole-based new fluorogenic differential/sequential  
chemosensor for Cu<sup>2+</sup>, Zn<sup>2+</sup>, CN<sup>-</sup>, P<sub>2</sub>O<sub>7</sub><sup>4-</sup>, DNA, its live-cell imaging and  
pyrosequencing applications**

**Sellamuthu Anbu,<sup>a,b,\*</sup> Anup Paul,<sup>a</sup> Kalpana Surendranath,<sup>c</sup> Nadeen Shaikh  
Solaiman,<sup>c</sup> Armando J. L. Pombeiro<sup>a</sup>**

<sup>a</sup>*Centro de Química Estrutural, Instituto Superior Técnico, Universidade de Lisboa, Av.  
Rovisco Pais, 1049-001 Lisboa. Portugal.*

<sup>b</sup>*Departments of Chemistry and Biomedical Sciences, Cottingham Road, University of  
Hull, Hull, HU6 7RX, United Kingdom.*

<sup>c</sup>*Genome Engineering Laboratory, School of Life Sciences, University of Westminster,  
W1W 6UW London, United Kingdom.*

---

**Abstract:** Differential chemosensors have emerged as next-generation systems due to their simplicity and favourable responsive properties to produce different signals upon selective binding of various analytes simultaneously. Nevertheless, given their inadequate fluorescence response and laborious synthetic procedures, only a few differential chemosensors have been developed so far. In this work, we have employed a single pot synthesis strategy to establish a new benzimidazole-based Schiff base type fluorogenic chemosensor (**DFB**) which differentially detects Cu<sup>2+</sup> (detection limit (LOD) = 24.4 ± 0.5 nM) and Zn<sup>2+</sup> (LOD = 2.18 ± 0.1 nM) through fluorescence “off-on” manner over the library of other metal cations in an aqueous medium. The **DFB**-derived ‘*in situ*’ complexes **DFB-Cu<sup>2+</sup>** and **DFB-Zn<sup>2+</sup>** showed fluorescence revival “on-off” responses toward cyanide (CN<sup>-</sup>) and bio-relevant pyrophosphate (P<sub>2</sub>O<sub>7</sub><sup>4-</sup>-PPi) ions with a significantly low LOD of 9.43 ± 0.2 and 2.9 ± 0.1 nM, respectively, in water. We have demonstrated the phosphate group-specific binding capability of **DFB-Zn<sup>2+</sup>**, by testing it

with both ssDNA and dsDNA samples which displayed fluorescence “*turn-off*” response (LOD  $\sim 10^{-7}$  M), similar to the PPI binding in an aqueous medium, indicating that it interacts explicitly with the phosphate backbone of DNA. We have also harnessed the **DFB** as a sequential fluorescent probe to detect  $\text{Cu}^{2+}$ ,  $\text{Zn}^{2+}$ ,  $\text{CN}^-$  and  $\text{P}_2\text{O}_7^{4-}$  ions in human cervical (HeLa) and breast (MCF-7 and MDA-MB-231 (aggressive and invasive)) cancer cell lines. Moreover, we have explored the PPI recognition capability of **DFB-Zn<sup>2+</sup>** in the polymerase-chain-reaction (PCR) products where PPI is one of the primary by-products during amplification of DNA.

Keywords: Benzimidazole, Differential  $\text{Cu}^{2+}$  and  $\text{Zn}^{2+}$  sensor, Cyanide and PPI-sensor, Metastatic cells, Metal-based DNA-sensor, PPI-detection in PCR products.

---

\*Corresponding author

E-mail: [bioinorg\\_anbu@yahoo.com](mailto:bioinorg_anbu@yahoo.com)

## 1. Introduction

Designing and development of chemosensors for bio-relevant metal cations are an emerging area of research in supramolecular chemistry [1]. This offers a lot of platforms to construct suitable materials for assessment of metal ion levels which influence diverse biological and environmental processes [2]. Amongst the several reported chemosensors, those based on the fluorescent recognition of metal ions have attracted considerable interest due to their simplicity, specificity, high sensitivity, and capability to monitor and convert the metal recognising event into the signals rapidly [1-5]. Notably, more efforts have been put forward on developing novel fluorogenic chemosensors for the detection of  $\text{Cu}^{2+}$  and  $\text{Zn}^{2+}$  ions since these metal ions are highly bio-relevant and involved in a range of environmental and biological processes [6-9].

$\text{Cu}^{2+}$  is one of the rifest transition metal ions present in the human body, responsible for diverse critical roles in various physiological reactions and energy transport processes [10]. The disruption in copper homeostasis is directly linked with neuron activation and severe neurodegenerative diseases like Alzheimer's, Wilson and Menkes diseases [11, 12]. For instance,  $\text{Cu}^{2+}$  acts as the active centre and co-factor for various metalloenzymes including superoxide dismutase, cytochrome oxidase and tyrosinase and their activities [13, 14]. Copper is also an essential micronutrient for plants, and it is needed for ensuring several central plant cellular processes, and excessive  $\text{Cu}^{2+}$  in the soil is associated with several deposition diseases, including chlorosis [15].

On the other hand,  $\text{Zn}^{2+}$  is another central metal ion which regulates relevant cellular functions, and it is present in more than 3000 putative human proteins [16, 17]. In the human brain, high concentrations (micromolar level) of chelatable intracellular  $\text{Zn}^{2+}$  ions are stored in the hippocampus, regulating the neuron communications to improve memory and learning capabilities [17, 18]. A large variety of zinc-based compounds have been explored as insulin-mimetic [19], tumour photosensitizers in photodynamic therapy

[20], biomedical imaging [21], radiation-induced damage protective [22], anticancer [23] and antiviral therapeutic (via nucleic acid interaction) agents [24]. Therefore, the detection and quantification of  $\text{Cu}^{2+}$  and  $\text{Zn}^{2+}$  levels in biological and environmental scenarios using fluorogenic chemosensors are of recognized significance.

Among the different anions recognitions of interest, that of  $\text{CN}^-$  ion in real and environmental samples has received increasingly great attention due to its lethal toxicity and extensive applications in metallurgy, plastics, fibres, dyes, water treatment and pharmaceuticals [25-29]. In recent years, several chemosensor systems for cyanide ion [25] detection have been developed which work via different sensing mechanistic modes, such as H-bonding [30], complexation [31], C-C (double) bond activation by nucleophilic addition [32], metal displacement from preassembled sensor systems [33-35] and so on. Among the analytical techniques, such as atomic absorption spectral [36], electrochemical [37] and colourimetric methods [35, 37, 39], the fluorescence detection of  $\text{CN}^-$  ion by  $\text{Cu}^{2+}$  based probes through metal displacement approach has many advantages including secure and fast response, high sensitivity, economical and accessibility in aqueous medium [33, 40, 41].

The inorganic pyrophosphate ( $\text{P}_2\text{O}_7^{4-}$ -PPi) is a by-product of DNA or RNA polymerization reactions, and this is the key for diverse metabolic processes including energy storage and transport, regulation of ion-channels, intercellular signalling arbitration, enzymatic including phosphorylation reactions and DNA-replication in the living systems [42-48]. The detection of PPi levels in synovial fluid and urine allows quantifying the calcium in the form of crystalline calcium pyrophosphate dehydrate, responsible for several bone joints diseases including chondrocalcinosis or pseudogout in the human body [49]. Furthermore, PPi is also essential for the sucrose synthase activity in the plants to develop starch stored seeds, and tubers through ADP-glucose PPase catalyzed the reaction [50]. The PPi levels in the cells can offer precise information on

DNA replication processes, and this can be used as a cancer biomarker since it is released during the telomerase elongation process which takes place in almost all human tumours but not in adjacent healthy tissues [51]. Thus, development of new chemosensors for phosphates opens up the opportunities to identify novel and promising diagnostic reagents for the genetic diseases and the monitoring of intracellular processes [52, 53].

Therefore, design and developing of a new generation chemosensor systems with selective and sensitive signalling units (fluorophores) for differential detection of  $\text{Cu}^{2+}$  and  $\text{Zn}^{2+}$ , as well as secondary recognition of anions (e.g.,  $\text{CN}^-$  and  $\text{PPi}$ ) by “*off-on*” manner, are a promising area that advances the chemosensor research into a next level. However, a single chemosensor which discriminatively recognizes the specific metal ions from others in “*off-on*” fashion is limited in the literature [3, 6-9, 54, 55]. Recently, we have also devoted to developing fluorogenic differential sensors for rapid recognition of  $\text{Cu}^{2+}$  and  $\text{Zn}^{2+}$  ions and the consequential detection of  $\text{S}^{2-}$  and  $\text{PPi}$  anions [7, 8]. Very recently, we have arrayed a range of chemosensors (totally 150) developed over a decade from 2010 to 2019 including metal-based and sequential sensors that selectively detect  $\text{PPi}$  in both environmental and biological scenarios [56].

Notably, the development of a fluorescent chemosensor for probing two different metal ions and significant detection of anions as well as biomolecules such as DNA in the aqueous medium through a single technique via exploring distinct fluorescence signals for the different analyte is challenging, and no such sensors have been reported so far. In the context of the above objectives, for the first time, we are reporting a benzimidazole-based Schiff base type fluorogenic chemosensor (**DFB**) for the differential detection of  $\text{Cu}^{2+}$  and  $\text{Zn}^{2+}$  ions by an “*off-on*” manner and its secondary sensor applications towards cyanide, pyrophosphate ions and DNA molecules. We have demonstrated the use of **DFB** as a sequential bioimaging probe for concomitant recognition of  $\text{Cu}^{2+}$ ,  $\text{Zn}^{2+}$  and  $\text{PPi}$  in

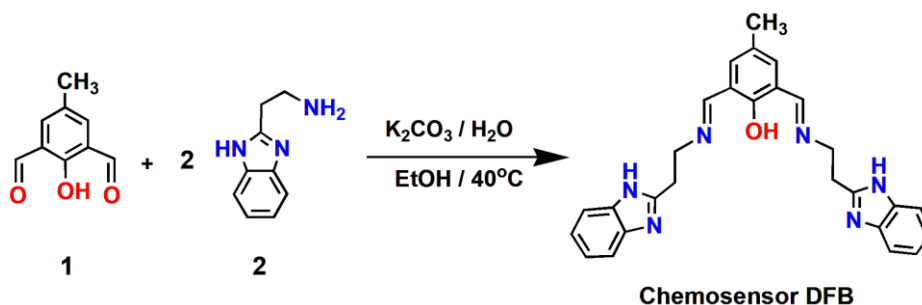
cultured human cervical (HeLa) and breast cancer (MCF-7 and MDA-MB 231 (invasive and aggressive)) cell lines and PCR amplified DNA product mixtures.

## 2. Results and Discussion

### 2.1. Synthesis and characteristic aspects of chemosensor **DFB**

We have employed a single pot strategy to develop a new fluorogenic chemosensor (**DFB**) (Scheme 1) by reacting (1H-benzo[d]imidazol-2-yl) ethanamine (**2**) and 2,6-diformyl-4-methyl phenol (**1**) in ethanol at 40 °C (See experimental details in Supporting Information, SI). This simple Schiff base type **DFB** acts as an excellent sensor for Cu<sup>2+</sup> and Zn<sup>2+</sup> ions, and its metal complexes serve as secondary probes for CN<sup>-</sup>, PPI and DNA in aqueous conditions. The molecular structures of the chemosensor **DFB** and its Cu<sup>2+</sup> and Zn<sup>2+</sup> complexes (**DFB-Cu<sup>2+</sup>** and **DFB-Zn<sup>2+</sup>**) are proved based on spectroscopic (FT-IR, <sup>1</sup>H, <sup>13</sup>C NMR) and ESI-MS data, and elemental analyses (Figs S1-S5). A highly symmetrical <sup>1</sup>H NMR spectrum was obtained for the chemosensor **DFB** (Fig. S1), in which two aromatics and three aliphatic sets of proton signals were consistent with its molecular structure. Other essential signals corresponding to the phenolic OH, benzimidazole NH and azomethine CH=N protons appeared at 14.01, 12.32 and 8.63 ppm, respectively, further confirming the formation of the Schiff base type compound **DFB** with N<sub>4</sub>O donors for metal binding. To prove the carbon skeleton of the **DFB**, we have recorded the <sup>13</sup>C NMR spectrum (Fig. S2) in DMSO-*d*<sub>6</sub>. Twelve signals, including eight for aromatic carbons, three resonances for aliphatic carbons and an intense signal at 163 ppm assigned to the azomethine carbon (C=N), were observed. An acetonitrile solution of **DFB** showed an intense (ESI-MS) peak at *m/z* = 451.44 (Fig. S3), which corresponds to the formation of [**DFB**+H<sup>+</sup>]<sup>+</sup>. A strong IR band observed at 1635 cm<sup>-1</sup>, characteristic of azomethine (C=N) stretching vibration, indicates the formation of a Schiff base between the dialdehyde and benzimidazole ethylamine. Notably, this critical band was significantly shifted to a higher wavenumber (1642 and 1641 cm<sup>-1</sup>) upon

forming  $\text{Cu}^{2+}$  and  $\text{Zn}^{2+}$  complexes, suggesting that the C=N nitrogens of **DFB** are involved in metal coordination. Moreover, both **DFB-Cu<sup>2+</sup>** and **DFB-Zn<sup>2+</sup>** display four bands in the UV region (260–550 nm) ascribed to the intra-ligand  $\pi$ - $\pi^*$  transitions within the phenolate oxygen and azomethine nitrogens of **DFB** in a  $\text{CH}_3\text{CN}/(50 \text{ mM})$  HEPES buffer at pH 7.4. The sensor-derived copper(II) complex **DFB-Cu<sup>2+</sup>** (Fig. S4) displays HRMS peaks at  $m/z = 296.03$ ,  $629.09$  and  $647.01$ , consistent with the  $[\text{Cu}_2(\text{DFB})(\text{OH})]^{2+}$ ,  $[\text{Cu}_2(\text{DFB})(\text{OH})(\text{Cl})]^+$  and  $[\text{Cu}_2(\text{DFB})(\text{H}_2\text{O})(\text{OH})(\text{Cl})]^+$  species, respectively, confirming the formation of a 1:2 complex. On the other hand, the complex **DFB-Zn<sup>2+</sup>** shows a major peak (Fig. S5) at  $m/z = 515.14$ , attributed to the existence of  $[\text{Zn}(\text{DFB})]^+$  species, which confirms the 1:1 (DFB:Zn<sup>2+</sup>) complex formation. All these data reveal the formation of the proposed Schiff base type chemosensor **DFB** and its  $\text{Cu}^{2+}$  and  $\text{Zn}^{2+}$  complexes (**DFB-Cu<sup>2+</sup>** and **DFB-Zn<sup>2+</sup>**) for sensor studies.



**Scheme 1** Synthesis of chemosensor **DFB**

## 2.2. Metal ion sensing studies

We have used  $^1\text{H-NMR}$ , absorption and fluorescence spectroscopic titration strategies (Fig. 1) to monitor the differential  $\text{Cu}^{2+}$  and  $\text{Zn}^{2+}$  detection capability of **DFB** in  $\text{CH}_3\text{CN}/50 \text{ mM}$  HEPES buffer at  $\text{pH} = 7.4$ . **DFB** ( $5 \mu\text{M}$ ) showed four prominent absorption bands at *ca.* 273, 280, 360 and 440 nm. Under a similar set of conditions, **DFB** displayed a weak fluorescence emission band *ca.* at 515 nm upon excitation at 380

nm. To confirm the dual selectivity and distinct sensitivity of the **DFB** toward  $\text{Cu}^{2+}$  and  $\text{Zn}^{2+}$  ions, we have titrated it with various metal ions such as  $\text{Hg}^{2+}$ ,  $\text{Cd}^{2+}$ ,  $\text{Ni}^{2+}$ ,  $\text{Co}^{2+}$ ,  $\text{Fe}^{2+}$ ,  $\text{Mn}^{2+}$ ,  $\text{Ca}^{2+}$ ,  $\text{Fe}^{3+}$ ,  $\text{Mg}^{2+}$ ,  $\text{K}^+$  and  $\text{Na}^+$ . Interestingly, the **DFB** showed no significant change in its initial absorption spectrum (Fig. 1A) upon addition of the metal ions as mentioned above except  $\text{Cu}^{2+}$  and  $\text{Zn}^{2+}$ , which elicited remarkable fluorescence quenching (9-fold) and significant fluorescence enhancement (4-fold) responses, respectively (Fig. 1B).

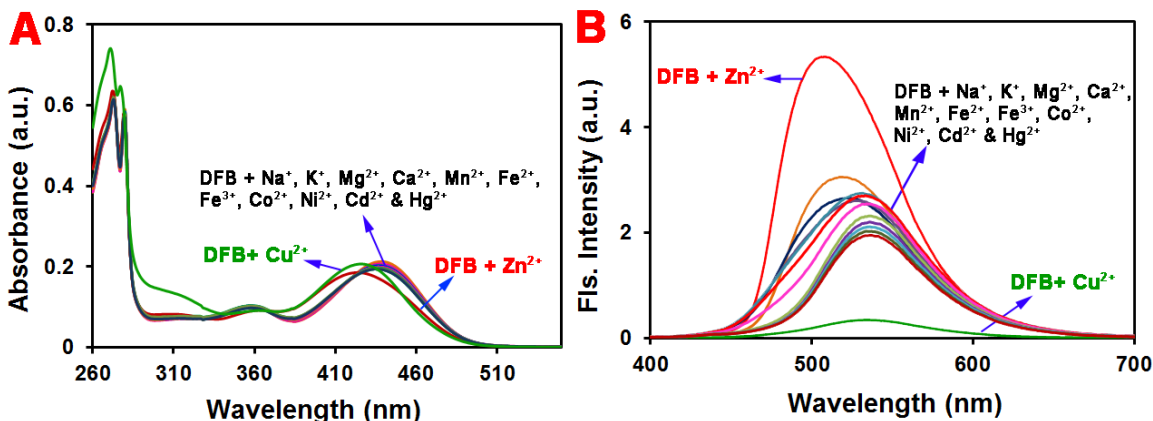


**Fig. 1.** Absorption (A) and fluorescence ( $\lambda_{\text{ex}} = 380$  and  $\lambda_{\text{em}} = 515$  nm) (B) spectral titrations of chemosensor **DFB** (5  $\mu\text{M}$ ) with different metal cations in  $\text{CH}_3\text{CN}/50$  mM HEPES buffer medium at  $\text{pH} = 7.4$ .

The initial absorption spectrum of **DFB** was dramatically changed upon incremental addition of  $\text{Cu}^{2+}$  (0–25  $\mu\text{M}$ ) or  $\text{Zn}^{2+}$  (0–15  $\mu\text{M}$ ). The absorption maximum at *ca.* 440 nm remarkably decreased along with a blue shift of *ca.* ~18 nm. This Stark blue shift is ascribed to the participation of the phenolate O-atom, part of the azomethine and benzimidazole N-atoms, in metal coordination [57, 58]. In both the  $\text{Cu}^{2+}$  and  $\text{Zn}^{2+}$  titration profiles, the absorption maxima at *ca.* 360 nm decreased along with the appearance of a new absorption band at *ca.* 308 nm, attributed to charge-transfer in complexes **DFB-Cu<sup>2+</sup>** and **DFB-Zn<sup>2+</sup>**. Four well distinct isosbestic points observed at *ca.* 284, 332, 369 and 434 nm for **DFB-Cu<sup>2+</sup>** and three points at *ca.* 284, 369 and 424 nm for

**DFB-Zn<sup>2+</sup>** agree with the existence of an equilibrium between chemosensor **DFB** and its appropriate metal complex **DFB-M<sup>2+</sup>** ( $M^{2+} = Cu^{2+}, Zn^{2+}$ ), in solution. The extent of  $Cu^{2+}$  or  $Zn^{2+}$  binding propensity ( $K_a$ ) of **DFB** was estimated as  $1.67 \times 10^{10} M^{-2}$  and  $1.5 \times 10^4 M^{-1}$  from the absorptions spectral titration profiles (Fig. 2 insets), indicating the formation of 1:2 and 1:1  $Cu^{2+}$  and  $Zn^{2+}$  complexes of **DFB**, respectively (Scheme 2).

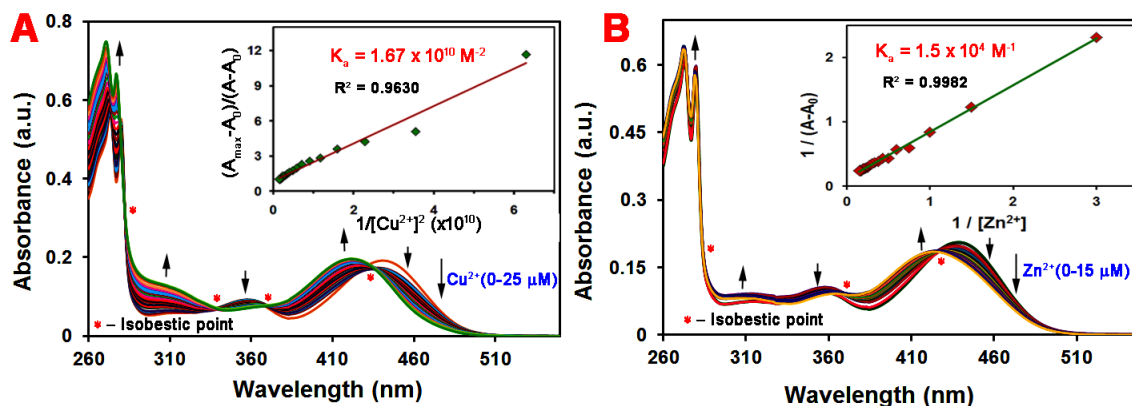


**Fig. 2.** Absorption spectral titration profiles of **DFB** (5  $\mu M$ ) with  $Cu^{2+}$  (0–25  $\mu M$ ) (A) and  $Zn^{2+}$  (0–15  $\mu M$ ) (B) ions in  $CH_3CN/50$  mM HEPES buffer at pH 7.4 (Insets show the linear Benesi-Hildebrand plots).

The moderate fluorescence emission at *ca.* 515 nm (Quantum yield,  $\Phi_f = 0.12$ ) of **DFB** is likely due to the presence of the ethyl spacer group which partially hampers the photoinduced electron transfer (PET) process between the benzimidazole fluorophore units and 2,6-diformyl-4-methyl phenol. Fig. 3A shows the change in the initial fluorescence intensity of **DFB** upon the gradual addition of an aqueous  $Cu^{2+}$  solution (0–20  $\mu M$ ). A small reduction of the initial emission intensity and significant redshift (530 nm) by *ca.*  $\sim 15$  nm was observed until the addition of an equivalent of  $Cu^{2+}$  ions. This initial little fluorescence “turn-off” found upon titration of 0-1 equivalent of  $Cu^{2+}$  ions is attributed to fractional mitigation of quenching as one binding compartment of **DFB** is occupied, leaving the other binding compartment to continue the photoinduced

electron transfer (**PET**) process (Scheme 2) [59]. A subsequent gradual treatment up to two equivalents of  $\text{Cu}^{2+}$  solution induces a strong quenching ( $\sim 8.8$  fold decrease) of the emission intensity at *ca.* 530 nm with a slight blue shift *ca.*  $\sim 3$  nm. Notably, the dramatic quenching of the fluorescence at *ca.* 530 nm reaches a plateau at *ca.* 2.4 equivalents ( $\sim 12$   $\mu\text{M}$ ) of  $\text{Cu}^{2+}$ . The apparent  $\text{Cu}^{2+}$  association constant ( $K_a$ ) was determined as  $1.63 \times 10^{10}$   $\text{M}^{-2}$  by plotting  $[(F_0 - F_{\text{min}})/(F_0 - F)]$  against  $1/[\text{Cu}^{2+}]^2$  (Fig. S6A). The significant redshift and concomitant quenching of emission intensity of **DFB** are endorsed to the reverse photoinduced electron transfer from the 4-methyl phenyl moiety to the phenolic-O, azomethine and benzimidazole-N atoms attributed to the decrease in electron density upon  $\text{Cu}^{2+}$  ion complexation [57, 58, 60, 61].

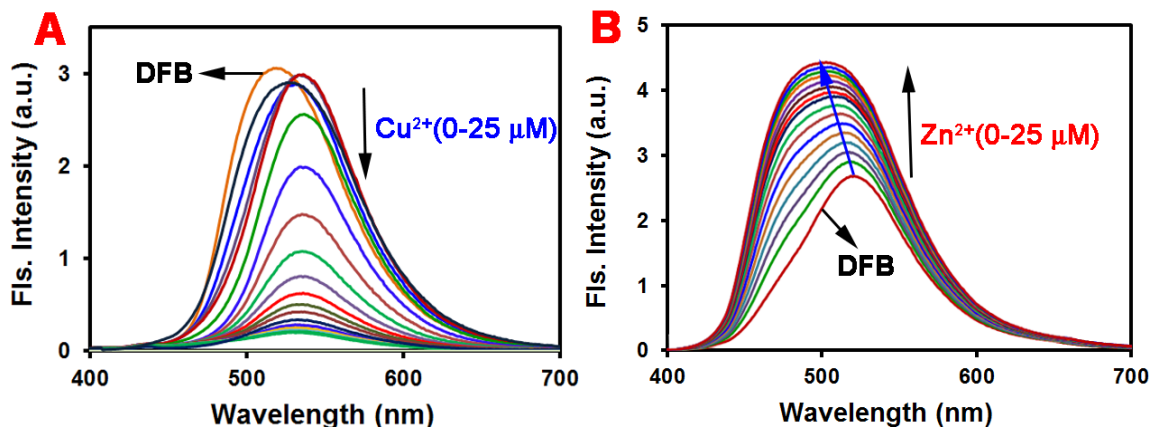


**Fig. 3.** Fluorescence spectral titration profiles of **DFB** (5  $\mu\text{M}$ ) versus  $\text{Cu}^{2+}$  (A) and  $\text{Zn}^{2+}$  (B) (0–25  $\mu\text{M}$ ), in  $\text{CH}_3\text{CN}$  / (50 mM) HEPES buffer medium at pH = 7.4. ( $\lambda_{\text{ex}} = 380$  and  $\lambda_{\text{em}} = 515$  nm).

On the other hand, the fluorescence emission of **DFB** at *ca.* 515 nm significantly increased ( $\sim 1.8$  fold increase) with a blue shift of  $\sim 10$  nm up to *ca.* 505 nm, after the addition of small aliquots ( $\sim 1.0$  equivalent) of  $\text{Zn}^{2+}$  ions (Fig. 3B). This remarkable fluorescence enhancement ( $\Phi_f = 0.21$ ) with a significant blue shift of **DFB-Zn<sup>2+</sup>** is attributed to the excimer interaction between benzimidazole units (Scheme 2) and the

diamagnetic  $\text{Zn}^{2+}$  ion which does not promote any electron- or energy-transition mechanisms for the deactivation of the excited state [62, 63] and inhibition of PET mechanism [57, 58] between donors and the  $\text{Zn}^{2+}$  ion. Moreover, the  $\text{Zn}^{2+}$  binding constant ( $K_a$ ) of **DFB** was determined as  $2.0 \times 10^4 \text{ M}^{-1}$  from the fluorescence titration profile for the plot of  $[1/(F-F_0)]$  against  $1/[\text{Zn}^{2+}]$  (Fig. S6B) using the modified linear Benesi–Hildebrand expression [60, 61]

To further confirm the binding mode and ratio of the chemosensor with  $\text{Zn}^{2+}$  (a diamagnetic metal ion), we have used the  $^1\text{H}$  NMR titration method to monitor the change in the initial  $^1\text{H}$ -NMR spectrum of chemosensor **DFB** upon gradual addition of  $\text{Zn}^{2+}$  in  $\text{DMSO-}d_6$  (Fig. S7). Aliquots of  $\text{Zn}^{2+}$  in  $\text{D}_2\text{O}$  (0.5, 1.0, 1.5 and 2.0 equivalents) were added to the  $\text{DMSO-}d_6$  solution of **DFB** (5 mM) and the  $^1\text{H}$ -NMR spectrum was recorded after each addition. The initial  $^1\text{H}$ -NMR spectrum of **DFB** gradually altered upon incremental addition of  $\text{Zn}^{2+}$ . In particular, the single broad resonance observed at  $\delta$  14.01 assigned to the phenolic OH disappeared after addition of 1 equivalent of  $\text{Zn}^{2+}$  indicating the **DFB** deprotonation upon metal binding. The other signals at 12.32 and 8.63 ppm corresponding to the metal ion binding site that comprises the benzimidazole NH and azomethine ( $\text{CH}=\text{N}$ ) protons ( $\delta$  in ppm), respectively, shifted to downfield considerably ( $\sim 0.3$ – $0.5$  ppm), suggesting that both donors were involved without deprotonation. The other signals due to aromatic and aliphatic protons become broadened with a little downfield shift after addition of an equivalent of  $\text{Zn}^{2+}$ , and this remains constant upon subsequent additions of (up to two equivalents) of  $\text{Zn}^{2+}$  ions. This confirms the participation of the  $\text{N}_4\text{O}$  donor site of chemosensor **DFB** for  $\text{Zn}^{2+}$  binding and the formation of the 1:1 stoichiometry complex, **DFB- $\text{Zn}^{2+}$** . Moreover, the stoichiometry plots (Fig. S8) based on the fluorescence spectral titration profiles also confirm the formation of 1:2 and 1:1 ratios of **DFB- $\text{Cu}^{2+}$**  and **DFB- $\text{Zn}^{2+}$** , respectively.

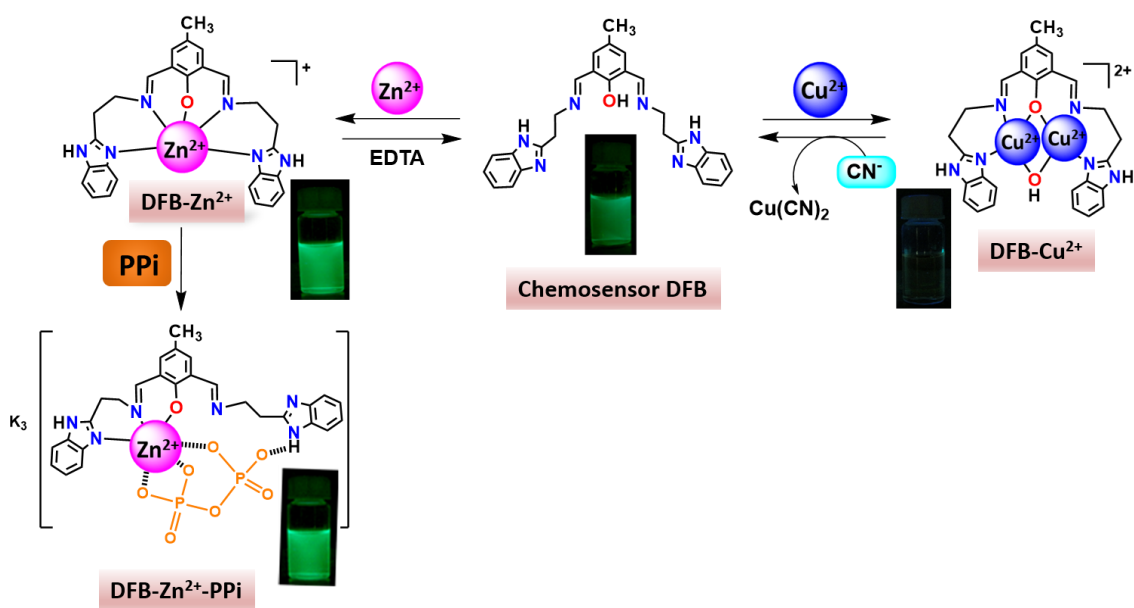
Furthermore, to confirm the distinct selectivity and sensitivity of **DFB** towards  $\text{Cu}^{2+}$  and  $\text{Zn}^{2+}$ , the interference of other metal has been examined by fluorescence titration with different metal ions such as  $\text{Hg}^{2+}$ ,  $\text{Cd}^{2+}$ ,  $\text{Ni}^{2+}$ ,  $\text{Co}^{2+}$ ,  $\text{Fe}^{2+}$ ,  $\text{Mn}^{2+}$ ,  $\text{Ca}^{2+}$ ,  $\text{Fe}^{3+}$ ,  $\text{Mg}^{2+}$ ,  $\text{K}^+$ , and  $\text{Na}^+$  ions (Figs. S9A and S9B). None of the metal ions elicits any considerable quenching response (green bars) except  $\text{Cu}^{2+}$  which induces efficient quenching of initial fluorescence of **DFB** (red bars). Notably, in the presence of  $\text{Cu}^{2+}$  ions, the fluorescence band at *ca.* 530 nm of **DFB** was significantly quenched even in the presence of  $\text{Zn}^{2+}$  ions revealing that the chemosensor **DFB** has a highly selective and sensitive binding capability towards  $\text{Cu}^{2+}$  over the other competing metal cations. This is attributed to the paramagnetic nature of  $\text{Cu}^{2+}$  that is capable of quenching the fluorescence emission of **DFB** through electronic or energy transformation during **DFB**- $\text{Cu}^{2+}$  formation [7]. Besides, upon addition of one equivalent of the sodium salt of EDTA solution to the *in situ* prepared **DFB**- $\text{Zn}^{2+}$  complex, the fluorescence intensity was almost reversed after 1 h of incubation (Fig. S9C). This revival of fluorescence suggests that **DFB** behaves as a reversible sensor system.

Moreover, based on the fluorescence spectral titration profiles of **DFB** with  $\text{Cu}^{2+}$  and  $\text{Zn}^{2+}$ , we have estimated the detection limits of **DFB** towards  $\text{Cu}^{2+}$  and  $\text{Zn}^{2+}$  as  $24.4 \pm 0.5$  nM and  $2.18 \pm 0.1$  nM, respectively (Figs. S10A and S10B). These are comparable to the values reported for other chemosensors for  $\text{Cu}^{2+}$  and  $\text{Zn}^{2+}$  ions [64-69] and adequate to recognize  $\text{Cu}^{2+}$  and  $\text{Zn}^{2+}$  ions in biological systems [70, 71].

### 2.3. Anion sensing studies

A single chemosensor system that is capable of recognising and showing distinct signals upon binding various analytes at a time is increasingly attractive [72]. In particular, chemosensor derived metal-based systems are relevant and useful for anion detection, given the possibility of exhibiting an improved water solubility and the availability of vacant coordination sites on metal ions [1]. Thus, the secondary anion sensing

capabilities of the *in situ* prepared  $\text{Cu}^{2+}$  and  $\text{Zn}^{2+}$  complexes (**DFB-Cu<sup>2+</sup>** and **DFB-Zn<sup>2+</sup>**) were investigated by both absorption and fluorescence spectral titration techniques. Initially, the selectivity and sensitivity of **DFB-Cu<sup>2+</sup>** toward a range of anions and phosphates including  $\text{CN}^-$ , PPI, Pi, ATP, AMP, ADP,  $\text{I}^-$ ,  $\text{Br}^-$ ,  $\text{Cl}^-$ ,  $\text{F}^-$ ,  $\text{CH}_3\text{COO}^-$ ,  $\text{CO}_3^{2-}$ ,  $\text{HCO}_3^-$ ,  $\text{N}_3^{3-}$  and  $\text{SO}_4^{2-}$  were investigated by both absorption and fluorescence spectral titration methods in  $\text{CH}_3\text{CN}/50$  mM HEPES buffer at  $\text{pH} = 7.4$ .



**Scheme 2** Possible detection modes of chemosensor **DFB**.

**DFB-Cu<sup>2+</sup>** displays a broad band centred at *ca.* 376 nm that comprises three humps at *ca.* 360, 385 and 405 nm characteristic of benzimidazole-based Schiff base compounds [73]. As shown in Fig. S11, the initial absorption spectrum of the dicopper(II) complex (**DFB-Cu<sup>2+</sup>**) drastically changed after addition of sodium salt of cyanide ( $\text{CN}^-$ ) ion, whereas any other of the above-listed anions induced significant changes. Notably, upon adding five equivalents of  $\text{CN}^-$  to the solution of **DFB-Cu<sup>2+</sup>**, the absorption band at *ca.* 376 nm was significantly decreased and largely shifted to longer wavelength to 435 nm. The  $\text{CN}^-$  ion

binding constant of **DFB-Cu<sup>2+</sup>** was estimated as ( $K_a = 9.9 \times 10^{10} \text{ M}^{-2}$ ) based on the changes being monitored in this absorption spectral band at 435 nm.

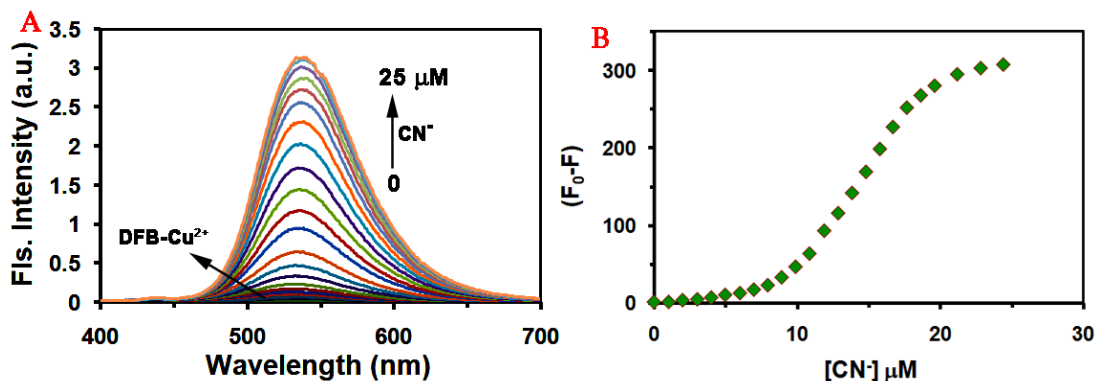


**Fig. 4.** (A) The fluorescence spectral titration profiles of **DFB-Cu<sup>2+</sup>** (5  $\mu\text{M}$ ) versus  $\text{CN}^-$  (0–25  $\mu\text{M}$ ) in  $\text{CH}_3\text{CN}$  / (50 mM) HEPES buffer medium at  $\text{pH} = 7.4$ . ( $\lambda_{\text{ex}} = 380$  and  $\lambda_{\text{em}} = 535$  nm). (B) Plot of change in the fluorescence emission of **DFB-Cu<sup>2+</sup>** at 535 nm as the function of  $\text{CN}^-$  concentration.

Under a similar set of conditions, in the presence of the anions mentioned above, the **DFB-Cu<sup>2+</sup>** (5  $\mu\text{M}$ ) showed no fluorescence emission enhancement except with  $\text{CN}^-$  ion which induced a dramatic enhancement (Fig. S12). Furthermore, competitive titration experiments of **DFB-Cu<sup>2+</sup>** versus different anions along with and without the presence of  $\text{CN}^-$  ions also confirm that the sensor can selectively recognize  $\text{CN}^-$  ion in a highly competitive manner. Interestingly, the initial non-fluorescent condition of **DFB-Cu<sup>2+</sup>** changed dramatically into a highly intense fluorescence band at 535 nm upon increasing addition of  $\text{CN}^-$  ions (Fig. 4A). This almost complete revival of the fluorescence emission along with the sigmoidal data points (Fig. 4B) suggest that the  $\text{Cu}^{2+}$  ions are consecutively sequestered (dicopper(II) **DFB-Cu<sup>2+</sup>** +  $2\text{CN}^- \Rightarrow \text{Cu}(\text{CN})_2$  + monocopper(II) **DFB-Cu<sup>2+</sup>**; monocopper(II) **DFB-Cu<sup>2+</sup>** +  $2\text{CN}^- \Rightarrow \text{Cu}(\text{CN})_2$  + **DFB**) as copper cyanide salt by  $\text{CN}^-$  ions with the release of the Cu-free chemosensor **DFB**. The  $\text{CN}^-$  anion binding plot analysis (Fig. S13) with an appreciable binding constant ( $K_a = 2.50 \times 10^{10} \text{ M}^{-2}$ ) and almost complete revival of fluorescence emission at 535 nm

(99.6%) confirms the formation of  $\text{Cu}(\text{CN})_2$  and metal-free **DFB** from the dicopper(II) complex **DFB-Cu<sup>2+</sup>**. Moreover, the **DFB-Cu<sup>2+</sup>** showed a remarkable  $\text{CN}^-$  detection limit ( $9.43 \pm 0.2 \times 10^{-9} \text{ M}$ ) (Fig. S14A), and it is higher than those of the reported literature of  $\text{Cu}^{2+}$ -based  $\text{CN}^-$  sensors [74-77], suggesting the potential use of our fluorescent probe for  $\text{CN}^-$  detection in both environmental and biological samples.

On the other hand, the **DFB** derived  $\text{Zn}^{2+}$ -complex **DFB-Zn<sup>2+</sup>** served as a secondary sensor for anions and displayed high selectivity and sensitivity toward PPI over other anions. This was reflected in absorption spectral selectivity experiments (Fig. S15A) where the main absorption band of **DFB-Zn<sup>2+</sup>** at *ca.* 405 nm was considerably shifted to a longer wavelength (420 nm) upon binding of PPI even in the presence of a range of the above listed common anions used for **DFB-Cu<sup>2+</sup>**. To ascertain the PPI binding propensity of **DFB-Zn<sup>2+</sup>** in the ground state, we have performed the absorption spectral titration of **DFB-Zn<sup>2+</sup>** with PPI in an aqueous medium (Fig. S15B). The **DFB-Zn<sup>2+</sup>** showed a very broadband centred at 405 nm. Upon increasing addition of PPI to a solution of **DFB-Zn<sup>2+</sup>**, the absorption maxima at *ca.* 405 nm slowly decreased along with a Stark redshift ( $\sim 25 \text{ nm}$ ). Analysis of the change in the initial absorption maxima ( $\text{Abs}_{405}/\text{Abs}_{425}$ ) of **DFB-Zn<sup>2+</sup>** ( $5 \mu\text{M}$ ) as a function of  $[\text{PPI}]$  (0-25  $\mu\text{M}$ ) using the nonlinear least-squares fitting allowed to determine the binding constant ( $K_{\text{PPI}}$ ) as  $2.4 \times 10^4 \text{ M}^{-1}$  (Fig. S16A).

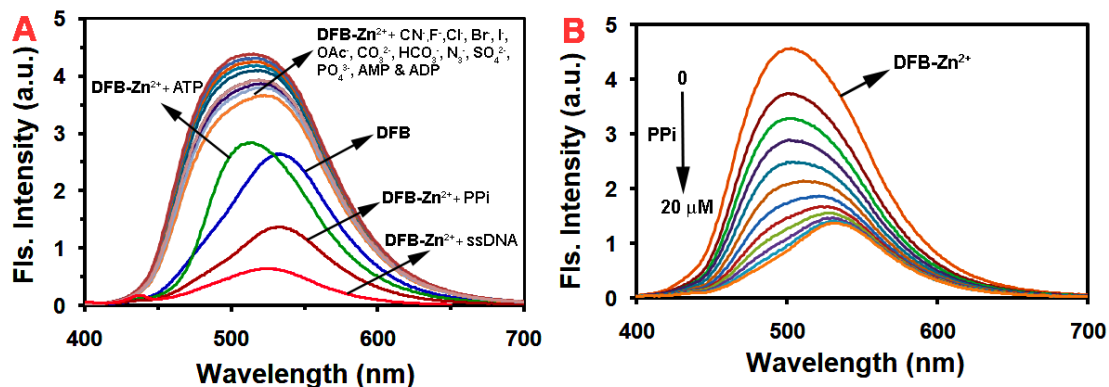


**Fig. 5.** (A) Fluorescence spectral profiles of **DFB** alone, and **DFB-Zn<sup>2+</sup>** ( $5 \mu\text{M}$ ) with and

without the presence of various anions including PPI and ssDNA (0–20  $\mu\text{M}$ ) in  $\text{CH}_3\text{CN}$  / (50 mM) HEPES buffer medium at  $\text{pH} = 7.4$ . ( $\lambda_{\text{ex}} = 380$  and  $\lambda_{\text{em}} = 505$  nm). (B) Titration of **DFB-Zn<sup>2+</sup>** (5  $\mu\text{M}$ ) versus PPI (0–20  $\mu\text{M}$ ) and inset showing the linear Benesi–Hildebrand plot of measured  $[1/(F-F_0)]$  at 505 nm as a function of  $1/[\text{PPI}]$ .

Under similar conditions, **DFB-Zn<sup>2+</sup>** (5  $\mu\text{M}$ ) showed an influential fluorescence band at *ca.* 505 nm upon exciting at 380 nm. This has almost remained the same in the presence of other anions and potentially interfering phosphates such as ADP and AMP and Pi, except the ATP and PPI which induced a significant quenching response. However, PPI elicits a dramatic quenching with a significant red shift of  $\sim 27$  nm (Fig. 5A). To further prove and ascertain the extent of selective PPI binding affinity of **DFB-Zn<sup>2+</sup>**, we have carried out the fluorescence titration experiments (Fig. 5B). Upon gradual addition of PPI concentration (0–20  $\mu\text{M}$ ) in the solution of **DFB-Zn<sup>2+</sup>** (5  $\mu\text{M}$ ), the initial fluorescent intensity at 505 nm was significantly attenuated ( $K_a = 1.1 \times 10^4 \text{ M}^{-1}$ ) with a Stark shift ( $\sim 27$  nm) to longer wavelength up to 532 nm (Fig. S16B). Notably, the extent of PPI induced quenching (83%) was higher than the fluorescent enhancement (73%) upon increasing concentration of **Zn<sup>2+</sup>** to the chemosensor **DFB**. This 10% efficient quenching indicates the formation of a new receptor-PPI (**DFB-Zn<sup>2+</sup>-PPI**) complex rather than the displacement of **Zn<sup>2+</sup>** ion from **DFB-Zn<sup>2+</sup>** as **Zn<sup>2+</sup>-PPI** complex and the metal-free chemosensor **DFB**. The weaker emission of the new **DFB-Zn<sup>2+</sup>-PPI** complex than the metal-free **DFB** is attributed to the weak force of interaction between chemosensor **DFB**, and **Zn<sup>2+</sup>** ion induces the reversal of PET process between donors in the metal-binding sites to the 4-methyl phenyl group. Besides, the NH groups presence in the benzimidazole arms of **DFB** also facilitates the intermolecular hydrogen bonding interaction with negatively charged oxygens of PPI, which modulates the PET mechanism [78], by altering the photophysical characteristics of fluorophores upon anion recognition.

The PPI interaction mode of receptor **DFB-Zn<sup>2+</sup>** was further ascertained by the <sup>31</sup>P-NMR method. The potassium salt of PPI (5 mM) in D<sub>2</sub>O showed a single <sup>31</sup>P resonance at  $\delta$  -6.20 (Fig. 6), which indicates that both the P nuclei of PPI are magnetically equal. However, this single signal was greatly perturbed, being replaced by two new broad signals at  $\delta$  -3.32 and -4.57 upon addition of one equivalent of **DFB-Zn<sup>2+</sup>** (5 mM). The significant downfield chemical shift values ( $\Delta\delta = -2.88$  and  $-1.63$  ppm) for the P-atoms (P<sub>a</sub> and P<sub>b</sub>) suggest that they are magnetically unequal [79], and the electron density around each P atom was reduced upon interaction with **DFB-Zn<sup>2+</sup>**. Based on these results, we postulate that the comparatively higher downfield shifted signal at -3.32 ppm concerns P<sub>a</sub>, which contributes with two oxygens for coordination, as shown in Fig. 6. The less shifted resonance at -4.57 ppm is assigned to P<sub>b</sub> with a shorter reduction of electron density, which likely interacts with the NH group of a benzimidazole moiety through one of the oxygens by hydrogen bonding. These results agree with the proposed structure (Scheme 2) of the new receptor-PPI complex (**DFB-Zn<sup>2+</sup>-PPI**).

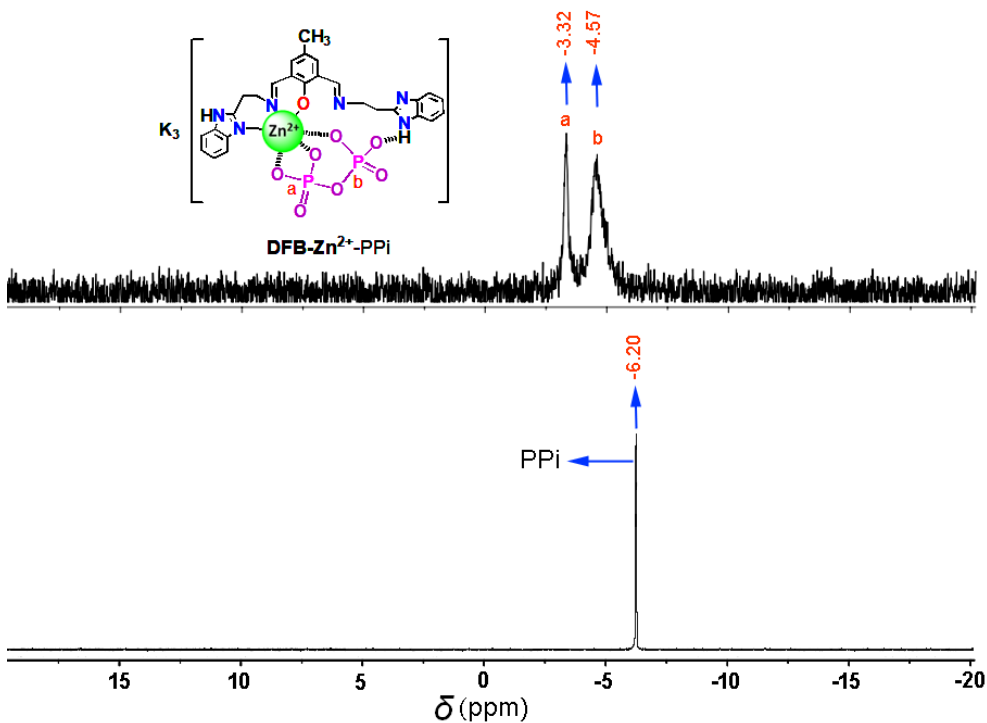


**Fig. 6.** <sup>31</sup>P NMR spectra of K<sub>4</sub>P<sub>2</sub>O<sub>7</sub> (5 mM) and **DFB-Zn<sup>2+</sup>** (5 mM) in D<sub>2</sub>O.

To substantiate the practical harnessing of **DFB-Zn<sup>2+</sup>** as the fluorescence PPI probe, we performed competitive titration experiments with other potentially competing anions Fig. S17. The initial fluorescence emission of **DFB-Zn<sup>2+</sup>** at *ca.* 505 nm underwent little or negligible fluctuations (blue bars) upon mixing with two equivalents of the other anions as mentioned above except for ATP which induced a significant quenching (35%). However, the successive addition of PPI (two equivalents) elicited a dramatic (80%) fluorescence quenching (green bars), which confirmed the high selectivity and sensitivity of **DFB-Zn<sup>2+</sup>** towards PPI over a range of potentially competing anions and organic phosphates in an aqueous medium. Moreover, we have used the PPI induced quenching effect to estimate the PPI detection limit of **DFB-Zn<sup>2+</sup>** as  $2.9 \pm 0.1 \times 10^{-9}$  M (1.76 ppb) (Fig. S14B), which is comparable to other reported Zn<sup>2+</sup>-based PPI sensors [80-83]. This indicates that **DFB-Zn<sup>2+</sup>** is an efficient PPI sensor which allowed to quantify the PPI level in biological samples (e.g. PPI concentration in human blood plasma = 1.19–5.65  $\mu$ M) [7, 84-86].

#### 2.4. DNA recognition studies

Development of chemosensors for nucleic acid recognition became increasingly attractive due to their diverse applications, including disease progression and diagnosis of early stages of cancer [87]. In particular, small molecule-like compounds can interact with macro-biomolecules such as nucleic acids in many ways, including intercalation ( $\pi$ - $\pi$ -interaction) between the base pairs, covalent, noncovalent, hydrophobic or electrostatic interaction [88]. Of particular significance are the metal-based systems with vacant coordination sites in their metal centres and overall positive charge which favours the noncovalent (electrostatic) interaction with negatively charged phosphate groups (backbone) of nucleic acids [89]. The encouraging results we accomplished from the PPI sensor experiments of **DFB-Zn<sup>2+</sup>** tempted us to harness this dicationic complex system to probe the DNA molecule. To demonstrate the DNA recognition capability of **DFB-Zn<sup>2+</sup>**,

we have carried out fluorescence titration experiments (Fig. 7) of **DFB-Zn<sup>2+</sup>** with two different single-stranded (random 19- and 20-mer) DNA sequences, *i.e.*, XOF (5'-GCATGACGTCATCGTCCTG-3'), XAPF (5'-GCAAGCTGATCGGTATCCTC-3') and a double-stranded (calf thymus) CT-DNA in CH<sub>3</sub>CN/Tris-HCl (50 mM NaCl) buffer medium at pH = 7.4.

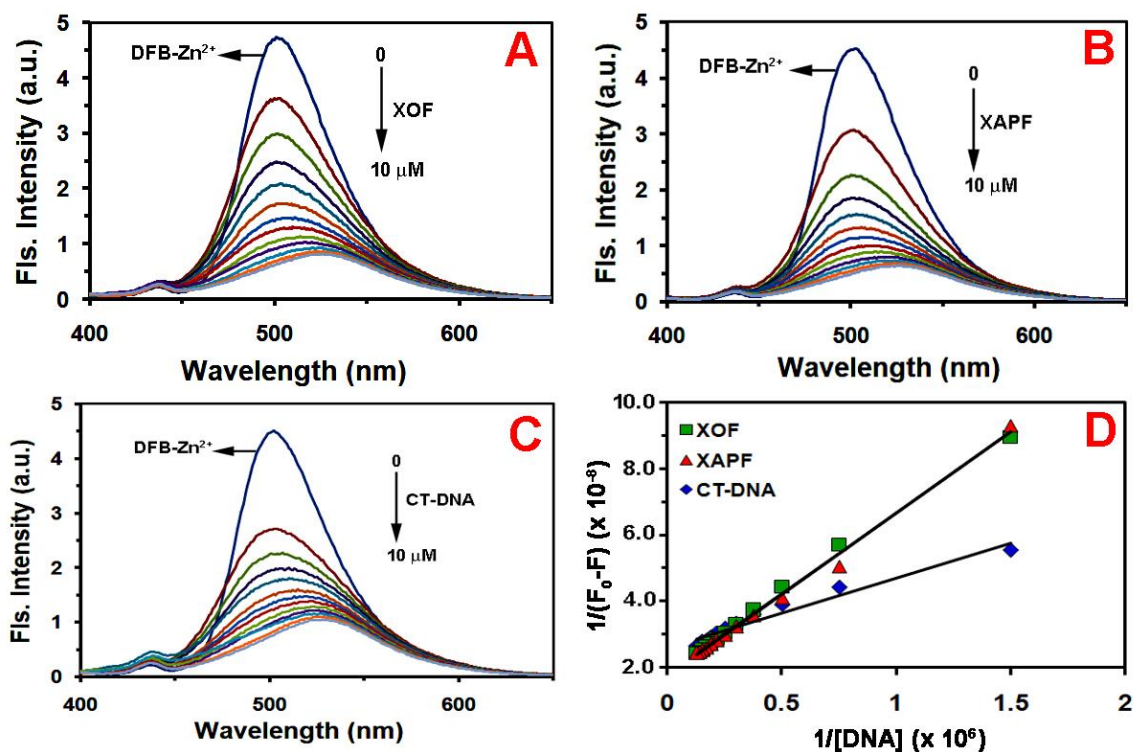


**Fig. 7.** (A-C) Change in the initial fluorescence spectrum of **DFB-Zn<sup>2+</sup>** (5 μM) upon gradual addition of ssDNA (XOF and XAPF) and CT-DNA (0–10 μM), respectively, in CH<sub>3</sub>CN/Tris-HCl (50 mM NaCl) buffer medium at pH = 7.4. (D) The linear Benesi–Hildebrand plot of  $[1/(F-F_0)]$  versus  $1/[DNA]$ .

As shown in **Fig. 7A-C**, the intense fluorescence emission of **DFB-Zn<sup>2+</sup>** (5 μM) at *ca.* 505 nm ( $\lambda_{ex} = 380$  nm) was dramatically attenuated (>85%) when adding aliquots of XOF, XAPF and CT-DNA solutions (0-10 μM). Both ssDNA and dsDNA (~2.0 equivalents) induced almost similar and strong fluorescence quenching (~6.0 fold decrease) with a Stark shift to the longer wavelength of 530 nm. These remarkable

quenching responses with a robust redshift (~25 nm) of **DFB-Zn<sup>2+</sup>** indicate the formation of new sensor-DNA complexes such as **DFB-Zn<sup>2+</sup>-XOF**, **DFB-Zn<sup>2+</sup>-XAPF** and **DFB-Zn<sup>2+</sup>-CT-DNA**, respectively, rather than the displacement of **Zn<sup>2+</sup>** from **DFB-Zn<sup>2+</sup>**. All these new sensor-DNA complexes are formed via electrostatic interaction between the dicationic sensor (**DFB-Zn<sup>2+</sup>**) and the negatively charged phosphate groups of DNA molecules consistent with the selective PPi binding experiment results and facilitate the PET process as observed in the **DFB-Zn<sup>2+</sup>-PPi** formation.

To ascertain the DNA binding propensity of **DFB-Zn<sup>2+</sup>**, we have plotted the reciprocal of fluorescence intensity variation against the reciprocal of DNA concentration ( $1/(F_0-F)$  versus  $1/[DNA]$ ) (Fig. 7D). The XOF, XAPF and CT-DNA binding constants ( $K_b$ ) of **DFB-Zn<sup>2+</sup>** are  $4.0 \times 10^5$ ,  $3.95 \times 10^5$  and  $1.5 \times 10^5 \text{ M}^{-1}$ , which agree with the fluorescence quenching responses of 86, 87 and 82%, respectively, obtained from the fluorescence spectral titration profiles. The significantly higher binding propensity and quenching responses of **DFB-Zn<sup>2+</sup>** toward ssDNA (XOF and XAPF) over ds(CT)DNA suggests that the sensor preferentially interacts with ssDNA since the negatively charged phosphate groups are more exposed to the solvent than in the case of ds-DNA [90, 91]. Besides, we have also determined the DNA detection limit values (LOD) of **DFB-Zn<sup>2+</sup>** for XOF, XAPF and CT-DNA (Fig. S18) from the titration profiles as  $5.5 \times 10^{-7}$ ,  $4.5 \times 10^{-7}$  and  $5.7 \times 10^{-7} \text{ M}$ , respectively, suggesting that it is an excellent Zn<sup>2+</sup>-based nucleic acid sensor.

### 2.5. Live-cell imaging

After identifying the nanomolar fluorescence (off-on responsive) detection capability of **DFB** toward Cu<sup>2+</sup> and Zn<sup>2+</sup> ions in an aqueous medium, we intended to use it as a fluorescent probe to detect the same ions in biological scenarios such as human cervical (HeLa) and breast (MCF-7 and MDA-MB 231 (invasive and aggressive)) and cancer cell lines *in vitro* (Figs. 8 and S19). We have used both live and fixed cell imaging strategies to verify the Cu<sup>2+</sup> and Zn<sup>2+</sup> recognition potentials of **DFB** under physiological conditions.

In the presence of chemosensor **DFB** (20  $\mu\text{M}$ ), cancer (HeLa, MCF-7 and MDA-MB 231), cell lines are significantly fluorescent (Figs. 8b, 8g and S19b).

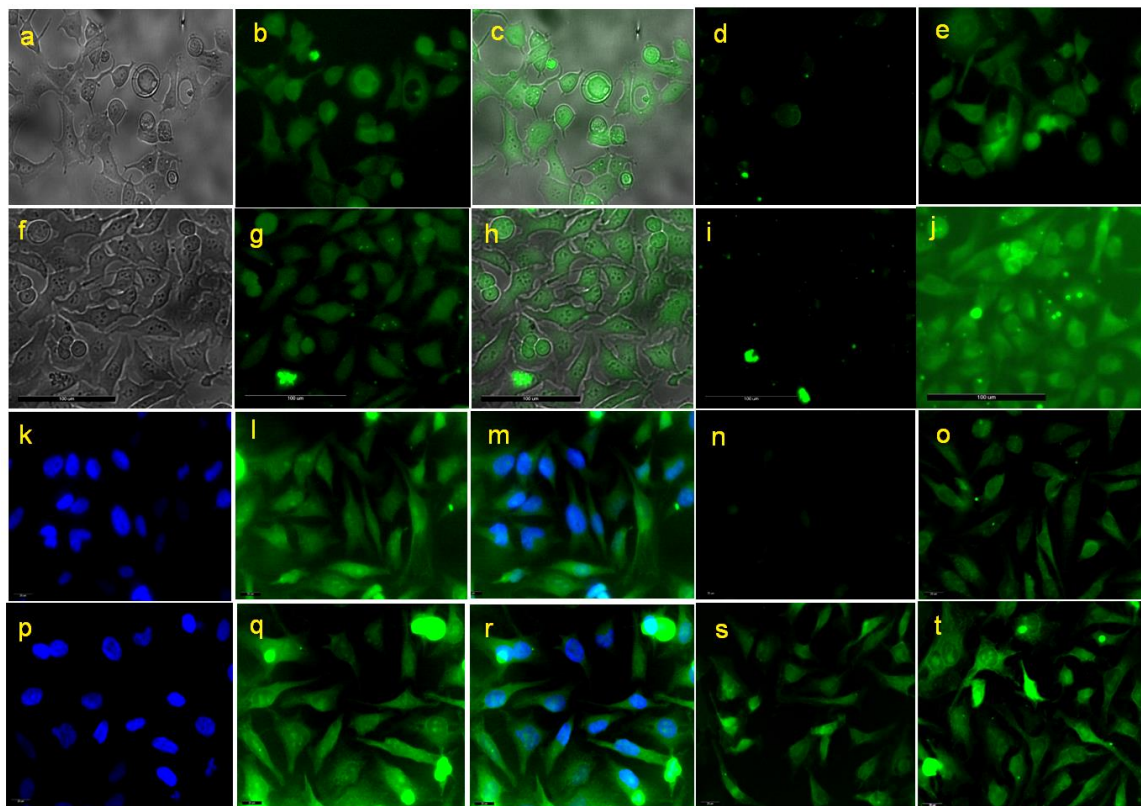


**Fig. 8.** (a-e and f-j) Live cell images of MCF-7 and HeLa cells, respectively, photographed by Olympus upright microscope: Bright field (a, c, f and h) and fluorescence images (b and c) of MCF-7 and HeLa cells incubated (2 h) with **DFB** (20  $\mu\text{M}$ ). Fluorescence images of MCF-7 and HeLa cells supplemented with **DFB** (20  $\mu\text{M}$ ) and two molar equivalents (40  $\mu\text{M}$ ) of  $\text{Cu}^{2+}$  (d and i) and  $\text{Zn}^{2+}$  (e and j). (k-t) Fluorescence images of HeLa cells (plated on coverslips in 6-well plates) imaged using 40x objective of Leica fluorescent microscope. (k and p) Fluorescence images of HeLa cells with DAPI as controls. i and q are the HeLa cells incubated (3 h) with **DFB** (20  $\mu\text{M}$ ) and **DFB- $\text{Zn}^{2+}$**  (20  $\mu\text{M}$ ) alone, respectively. The images m and r are the composite fluorescent images of k-l and p-q, respectively. The images n and o are the images of HeLa cells incubated with **DFB** (20  $\mu\text{M}$ ) +  $\text{Cu}^{2+}$  (40  $\mu\text{M}$ ) and **DFB** (20  $\mu\text{M}$ ) +  $\text{Cu}^{2+}$  (40  $\mu\text{M}$ ) + EDTA (40  $\mu\text{M}$ ), respectively. The images s and t are the images of HeLa cells incubated with **DFB** (20  $\mu\text{M}$ ) +  $\text{Zn}^{2+}$  (20  $\mu\text{M}$ ) + PPI (20  $\mu\text{M}$ ) and **DFB** (20  $\mu\text{M}$ ) +  $\text{Zn}^{2+}$  (20  $\mu\text{M}$ ) + EDTA (20  $\mu\text{M}$ ), respectively.

However, this has been quenched almost completely upon incubation with **DFB** and two molar equivalents of  $\text{Cu}^{2+}$ , indicating that **DFB** exhibits  $\text{Cu}^{2+}$  responsive potential in living cells. On the other hand, cells (Figs. 8e and 8j) supplemented with equimolar amounts of **DFB** and  $\text{Zn}^{2+}$  display enhanced fluorescence confirming biological  $\text{Zn}^{2+}$  detection capability of the sensor. Similarly, the observations in fixed (HeLa) cell imaging experiments (**DFB** with and without the presence of  $\text{Cu}^{2+}$  and  $\text{Zn}^{2+}$  ions (Figs. 8k-o, 8p-t and S19d-o) are also consistent with the results of live (HeLa and MDA-MB 231) cell imaging (Figs. 8f-j and S19a-c) and physicochemical sensor studies. In addition, the PPI imaging capability of 'in situ' generated monozinc(II) complex of **DFB**, *i.e.*, **DFB-Zn<sup>2+</sup>**, was examined in the presence of an equimolar amount of PPI. The marginal decrease in fluorescence in the HeLa and MDA-MB 231 cells (Fig. 8s and S19m-o) indicates the potential detection of PPI by **DFB-Zn<sup>2+</sup>** under physiological conditions. Notably, the fluorescence in the HeLa cells incubated with **DFB** +  $\text{Cu}^{2+}$  or **DFB** +  $\text{Zn}^{2+}$  ions were almost completely reversible upon addition of an equimolar amount of a benchmark chelating agent such as EDTA (rather than using lethally toxic  $\text{CN}^-$ ). These results show that **DFB** is a reversible sensor which gains access to both the cytosolic and nuclear compartments. Interestingly, the experiments discussed to demonstrate the potential of the probe in further applications, including elucidating the PPI mechanism through the ectonucleotide pyrophosphatase (Enpp1) enzyme levels overexpressed in breast cancer metastatic cells [92]. Taken together, our studies propose that **DFB** is a potential sequential multianalyte ( $\text{Cu}^{2+}$ ,  $\text{Zn}^{2+}$  and PPI) imaging agent to ascertain their biological activity in living cells.

#### 2.6. Pyrophosphate (PPI) detection in PCR amplified DNA mixtures

In recent years, PPI is considered as one of the potential biomarkers for various diseases including cancer, infectious and arthritis [93-96], since micromolar levels of PPI are present in the plasma of healthy adults [86]. Pyrosequencing is also a vital method to

recognise single nucleotide changes in genetic disorders in humans and pathogens, including somatic variations (low-level) caused by DNA point mutations in human genes that lead to cancer [97]. Also recently, the method is shown to increase accuracies of diagnosis of respiratory pathogens, including SARS-CoV-2 [98]. In principle, PPI is one of the primary by-products of the DNA polymerase reaction in PCR. It is essential for pyrosequencing (DNA sequence-by-synthesis strategy) and is often recognised by a fluorescent method using suitable sensors with fluorophores [97, 99, 100]. We also have developed fluorogenic  $Zn^{2+}$ -based probes to detect PPI in the polymerase chain reaction (PCR) product mixtures [84, 85].

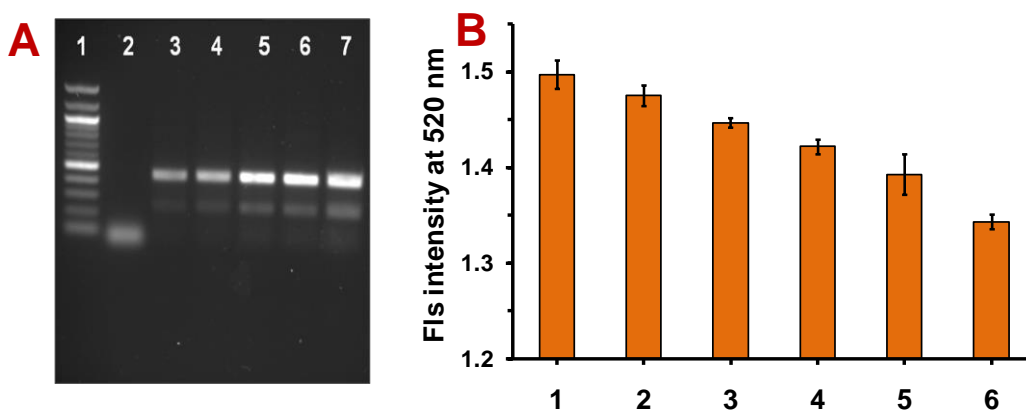


**Fig. 9.** (A) Gel (1.5% ultrapure agarose) electrophoresis diagram of PCR amplified DNA mixtures (left-right). (1) 100 bp NEB ladder, (2) negative control without the template, 10  $\mu$ L of the finished PCR product mixture (a 440 bp target site on the human genome was amplified using Taq polymerase and specific primers) performed with template DNA after (3) 29 cycles, (4) 30 cycles, (5) 31 cycles, (6) 32 cycles, and (7) 35 cycles. (B) Change in the fluorescence intensity of **DFB-Zn<sup>2+</sup>** at 520 nm upon addition of the PCR product mixtures obtained from the different PCR cycles 29, 30, 31, 32 and 35, respectively.

Although the initial fluorescence intensity of the **DFB** derived  $Zn^{2+}$  complex (**DFB-Zn<sup>2+</sup>**) at 520 nm (Fig. 5) was decreased considerably (~80%) upon selective binding of PPI over a range of other potentially interfering phosphates including ATP, still, it can be used to ascertain the PPI levels in PCR products. Therefore, we intended to use **DFB-**

$\text{Zn}^{2+}$  as a PPI recognising probe in PCR amplified DNA product mixtures. The gel electrophoresis diagram (Fig. 9A) confirms that the DNA production with the same molecular weight is increased with increasing the number of PCR cycles in which band intensity is directly proportional to the amount of PPI liberated during PCR. To further prove the PCR released PPI detection of **DFB-Zn<sup>2+</sup>**, the PCR products obtained from different cycles were incubated with **DFB-Zn<sup>2+</sup>** (0.5 mM) and the change in the fluorescence intensity at 520 nm was recorded. As expected, the fluorescence intensity at 520 nm corresponding to the sensor **DFB-Zn<sup>2+</sup>** decreased considerably (~50%) with increasing the number of PCR cycles. This implies that **DFB-Zn<sup>2+</sup>** is a potential PPI fluorescent probe used in new generation pyrosequencing strategies to ascertain the PPI levels in the biological scenarios.

### *2.7. Comparison of sequential recognition ( $\text{Cu}^{2+}/\text{Zn}^{2+}$ , $\text{CN}^-/\text{PPI}$ and DNA) capability of reported chemosensors with **DFB***

In order to explore the unique multi-analyte ( $\text{Cu}^{2+}$ ,  $\text{Zn}^{2+}$ ,  $\text{CN}^-$ , PPI and DNA) fluorescence responsive ability of the simple Schiff base type benzimidazole-based chemosensor **DFB**, we have performed a comparative analysis of previously reported sequential sensors (Table S1) [101-112]. Although most of the listed chemosensors (**C1-C3** and **C5-C12**) detected both metal ions and anions, none of them can simultaneously recognize more than one anion at a time similar to the proposed chemosensor **DFB** discussed in this paper. Notably, one of the reported Schiff base type sensors (**C4** developed by our group in 2015) showed ‘off-on-off’ fluorescence responses toward  $\text{Cu}^{2+}$ ,  $\text{Zn}^{2+}$  and PPI, respectively. However, the ‘turn-off’ response of the **C4**-derived  $\text{Zn}^{2+}$  complex (**C4-Zn<sup>2+</sup>**) towards PPI over other anions and nucleotide phosphates was attributed to the modulated PET mechanism. Several showcased sensor systems such as **C3**, **C5**, **C6** and **C7** possess simultaneous  $\text{Cu}^{2+}/\text{Zn}^{2+}$  ions and PPI/ $\text{CN}^-$  detection capability. However, they liberate the chemosensor back upon forming the metal-anion

complex ( $M^{2+}$ -PPI or  $M^{2+}$ -(CN)<sub>2</sub>) rather than the formation of PPI/CN<sup>-</sup> bound chemosensor-Cu<sup>2+</sup>/Zn<sup>2+</sup> complex. This was attributed to weaker binding interaction between Cu<sup>2+</sup>/Zn<sup>2+</sup> ions and chemosensors (**C3**, **C5**, **C6** and **C7**) than metal (Cu<sup>2+</sup>/Zn<sup>2+</sup>) ions and PPI/CN<sup>-</sup> which lead to leaching of metal ions from the chemosensor-derived Cu<sup>2+</sup>/Zn<sup>2+</sup>-complexes. More specifically, we have isolated chemosensor-derived Cu<sup>2+</sup> and Zn<sup>2+</sup> complexes (**DFB-Cu<sup>2+</sup>** and **DFB-Zn<sup>2+</sup>**). Both of them are water-soluble, and the latter dimeric complex was harnessed as a fluorescence probe to detect the PPI levels in PCR amplified DNA mixtures.

#### 4. Conclusions

We have designed and developed a new benzimidazole fluorophore appended Schiff base type chemosensor **DFB** by employing a single pot synthesis strategy. The **DFB** serves as excellent differential chemosensor, which displays “*off-on*” fluorescence responses toward Cu<sup>2+</sup> (LOD = 24.4 nM) and Zn<sup>2+</sup> (LOD = 2.4 nM), respectively, in aqueous medium. Also, we have generated **DFB**-derived *in situ* Cu<sup>2+</sup> and Zn<sup>2+</sup> complexes, **DFB-Cu<sup>2+</sup>** and **DFB-Zn<sup>2+</sup>**, and used them as secondary sensors for anions and nucleic acid recognition in an aqueous medium, in which they formerly displayed highly selective fluorescence “*turn-on*” response upon selective detection of CN<sup>-</sup> (LOD = 9.43 nM) over a range of other competitive anions. On the other hand, the **DFB-Zn<sup>2+</sup>** sensor system displayed a highly selective and sensitive fluorescence response toward PPI (LOD = 2.9 nM) even in the presence of potentially interfering other anions and phosphates including ATP, ADP, AMP in an aqueous medium. The Schiff base type chemosensor **DFB** acts as a promising sequential fluorescent imaging probe including concomitant detection potential of Cu<sup>2+</sup>, Zn<sup>2+</sup> and PPI in live-cell imaging of cultured cancer cells. More importantly, the sensor derived Zn<sup>2+</sup> complex (**DFB-Zn<sup>2+</sup>**) shows potential to detect PPI in metastatic, aggressive (human) breast cancer (MDA-MB 231) cells and found in PCR amplified DNA product mixtures.

Moreover, to the best of our knowledge, for the first time, we have used a simple Schiff base type chemosensor for recognising nucleic acids (ssDNA and dsDNA) and found that the **DFB-Zn<sup>2+</sup>** sensor can form a **DFB-Zn<sup>2+</sup>-ssDNA/dsDNA** complex via electrostatic interaction between the sensor and phosphate backbone of the DNA, in an aqueous medium.

Overall, **DFB** is a simple, economical, portable and excellent chemosensor capable of detecting both Cu<sup>2+</sup> and Zn<sup>2+</sup> ions simultaneously. The **DFB** derived metal complexes also can be used as secondary sensors for CN<sup>-</sup> and PPI/DNA, in an aqueous medium, showing distinct fluorescence signals.

### **Declaration of Competing Interest**

The authors declare that they have no known competing financial interests or personal relationships that could have appeared to influence the work reported in this paper.

### **Acknowledgement**

This work was partially supported by the Fundação para a Ciência e Tecnologia (FCT), Portugal, through project UIDB/00100/2020 of Centro de Química Estrutural. S.A. gratefully acknowledges the RSC for the Research Fund grant (RF19-7464), FCT for the award of postdoctoral fellowship (Ref.: SFRH/BPD/76451/2011) and the Department of Chemistry, the University of Hull, United Kingdom, for providing instrument facility to carrying out the HRMS analysis of the sensor-derived metal complexes. A.P. is thankful to the FCT and IST, Portugal, for financial support through “DL/57/2017” (Contracts no. IST-ID/197/2019). Work of the Genome Engineering Laboratory is supported by Quintin Hogg Trust “Gene Editors of the Future” and the University of Westminster, London, United Kingdom.

### **Appendix A. Supplementary data**

Supplementary material related to this article can be found in the online version.

## References

- [1] D. Wu, A. C. Sedgwick, T. Gunnlaugsson, E. U. Akkaya, J. Yoon, T. D. James, Fluorescent chemosensors: the past, present and future, *Chem. Soc. Rev.* 46 (2017) 7105–7123.
- [2] N. Kwon, Y. Hu, J. Yoon, Fluorescent chemosensors for various analytes including reactive oxygen species, biothiol, metal ions, and toxic gases, *ACS Omega* 3 (2018) 13731–13751.
- [3] R. Chandra, A. Ghorai, G. K. Patra, A simple benzildihydrazone derived colorimetric and fluorescent ‘on–off-on’ sensor for sequential detection of copper(II) and cyanide ions in aqueous solution, *Sensors and Actuators B* 255 (2018) 701–711.
- [4] N. De Acha, C. Elosúa, J. M. Corres, F. J. Arregui, Fluorescent sensors for the detection of heavy metal ions in aqueous media, *Sensors (Basel)*. 19 (2019) 599.
- [5] J. Harathi, K. Thenmozhi, *Mater. Chem. Front.* 4 (2020) 1471–1482.
- [6] M. S. Kim, T. G. Jo, H. M. Ahn, C. Kim, A colorimetric and fluorescent chemosensor for the selective detection of  $\text{Cu}^{2+}$  and  $\text{Zn}^{2+}$  ions, *J. Fluoresc.*, 27 (2016) 357–367.
- [7] A. Paul, S. Anbu, G. Sharma, M. L. Kuznetsov, M. F. C. Guedes da Silva, B. Koch, A. J. Pombeiro, Intracellular detection of  $\text{Cu}^{2+}$  and  $\text{S}^{2-}$  ions through a quinazoline functionalized benzimidazole-based new fluorogenic differential chemosensor, *Dalton Trans.* 44 (2015) 16953–16964.
- [8] S. Anbu, R. Ravishankaran, M. F. C. Guedes da Silva, A. A. Karande, A. J. L. Pombeiro, Differentially Selective Chemosensor with Fluorescence Off–On Responses on  $\text{Cu}^{2+}$  and  $\text{Zn}^{2+}$  Ions in Aqueous Media and Applications in Pyrophosphate Sensing, Live Cell Imaging, and Cytotoxicity. *Inorg. Chem.* 53 (2014) 6655–6664.
- [9] W.-N. Wu, H. Wu, Y. Wang, X.-J. Mao, B.-Z. Liu, X. -L. Zhao, Z. -Q. Xu, Y. -C. Fan, Z.-H. Xu, A simple hydrazone as a multianalyte ( $\text{Cu}^{2+}$ ,  $\text{Al}^{3+}$ ,  $\text{Zn}^{2+}$ ) sensor at different pH values and the resultant  $\text{Al}^{3+}$  complex as a sensor for  $\text{F}^-$ , *RSC Adv.* 8 (2018) 5640–5646.
- [10] H. Tapiero, D.M. Townsend, K. D. Tew, Trace elements in human physiology and pathology. *Copper, Biomed. Pharmacother.* 57 (2003) 386–398.
- [11] V. Desai, S. G. Kaler, Role of copper in human neurological disorders, *Am. J. Clin. Nutr.* 88 (2008) 855S–858S.
- [12] J. Kardos, L. Héja, Á. Simon, I. Jablonkai, R. Kovács, K. Jemnitz, *Cell Commun Signal.* 16 (2018) 71.
- [13] J. Osredkar, N. Sustar, Copper and Zinc, biological role and significance of copper/zinc imbalance, *J Clin Toxicol* (2011) S3; 001.
- [14] E. I. Solomon, D. E. Heppner, E. M. Johnston, J. W. Ginsbach, J. Cirera, M. Qayyum, M. T. Kieber-Emmons, C. H. Kjaergaard, R. G. Hadt, L. Tian, Copper Active Sites in Biology, *Chem. Rev.* 114 (2014) 3659–3853.

- [15] I. Yruela, Copper in plants, *Braz. J. Plant Physiol.* 17 (2005) 145-156.
- [16] Z. Pan, S. Choi, H. Ouadid-Ahidouch, J. -M. Yang, J. H. Beattie, and I. Korichneva, Zinc transporters and dysregulated channels in cancers, *Front Biosci (Landmark Ed)*. 22 (2017) 623–643.
- [17] H. Tamano, Y. Koike, H. Nakada, Y. Shakushi and A. Takeda, Significance of synaptic  $Zn^{2+}$  signaling in zincergic and non-zincergic synapses in the hippocampus in cognition, *J. Trace Elements in Med. and Biol.* 38 (2016) 93–98.
- [18] A. Takeda, H. Tamano, Innervation from the entorhinal cortex to the dentate gyrus and the vulnerability to  $Zn^{2+}$ , *J. Trace Elements in Med. and Biol.* 38 (2016) 19–23.
- [19] H. Sakurai, Y. Adachi, The Pharmacology of the Insulinomimetic Effect of Zinc Complexes, *BioMetals* 18 (2005) 319–323.
- [20] H. Abrahamse, M. R. Hamblin, New photosensitizers for photodynamic therapy, *Biochem J.* 473 (2016) 347–364.
- [21] E. Tomat, S. J. Lippard, Imaging Mobile Zinc in Biology, *Curr. Opin. Chem. Biol.* 14 (2010) 225–230.
- [22] S. J. Hosseinimehr, The protective effects of trace elements against side effects induced by ionizing radiation, *Radiat. Oncol. J.* 33 (2015) 66–74.
- [23] D. Skrajnowska, B. B.-Korczak, Role of Zinc in Immune System and Anti-Cancer Defense Mechanisms, *Nutrients* 11 (2019) 2273.
- [24] D. Garg, B. E. Torbett, Advances in targeting nucleocapsid-nucleic acid interactions in HIV-1 therapy, *Virus Res.* 193 (2014) 135–143.
- [25] F. Wang, L. Wang, X. Chen, J. Yoon, Recent progress in the development of fluorometric and colorimetric chemosensors for detection of cyanide ions, *Chem. Rev.* 43 (2014) 4312–4324.
- [26] L. Nelson, Acute Cyanide Toxicity: Mechanisms and manifestations, *Journal of Emergency Nursing: JEN: Official Publication of the Emergency Department Nurses Association* 32 (2006) S8–S11.
- [27] J. Lv, Z. Zhang, J. Li and L. Luo, A micro-chemiluminescence determination of cyanide in whole blood, *Forensic Sci. Int.* 148 (2005) 15–19.
- [28] M. A. Acheampong, R. J. W. Meulepas, P. N. L. Lens, Removal of heavy metals and cyanide from gold mine wastewater, *J. Chem. Tech. & Biotech.* 85 (2010) 590–613.
- [29] L. Yuan, W. Lin, Y. Yang, J. Song, J. Wang, Rational Design of a Highly Reactive Ratiometric Fluorescent Probe for Cyanide, *Org. Lett.* 13 (2011) 3730–3733.
- [30] H. Miyaji, J. L. Sessler, Off-the-Shelf Colorimetric Anion Sensors This research was supported by the National Institutes of Health (grant GM 58907) and the Texas Advanced Research Program, *Angew. Chem. Int. Ed.* 40 (2001) 154–157.
- [31] P. Xing, Y. Xu, H. Li, S. Liu, A. Lu, S. Sun, Ratiometric and colorimetric near-infrared sensors for multi-channel detection of cyanide ion and their application to measure  $\beta$ -glucosidase, *Scientific Reports* 5 (2015) 16528.

- [32] S.-J. Hong, J. Yoo, S.-H. Kim, J.S. Kim, J. Yoon and C.-H. Lee,  $\beta$ -Vinyl substituted calix[4]pyrrole as a selective ratiometric sensor for cyanide anion, *Chem. Commun.* (2009) 189–191.
- [33] L. Tang, P. Zhou, K. Zhong, S. Hou, Fluorescence relay enhancement sequential recognition of  $\text{Cu}^{2+}$  and  $\text{CN}^-$  by a new quinazoline derivative, *Sensors and Actuators B* 182 (2013) 439–445.
- [34] Y.-Y. Guo, X. -L. Tang, F. -P. Hou, J. Wu, W. Dou, W. -W. Qin, J. -X. Ru, G. -L. Zhang, W.-S. Liu, X. -J. Yao, A reversible fluorescent chemosensor for cyanide in 100% aqueous solution, *Sensors and Actuators B* 181 (2013) 202–208.
- [35] T. G. Jo, Y. J. Na, J. J. Lee, M. M. Lee, S. Y. Lee, C. Kim, A multifunctional colorimetric chemosensor for cyanide and copper(II) ions, *Sensors and Actuators B* 211 (2015) 498–506.
- [36] T. Wen, F. Qu, N. B. Li, H. Q. Luo, A facile, sensitive, and rapid spectrophotometric method for copper(II) ion detection in aqueous media using polyethyleneimine. *Arab. J. Chem.* 10 (2017) 10, S1680–S1685.
- [37] E. Karakuş, S. Gunduz, L. Liv, T. Ozturk, *J. Photochem. & Photobio. A: Chem.*, Fluorescent and electrochemical detection of Cu(II) ions in aqueous environment by a novel, simple and readily available AIE probe, 400 (2020) 112702.
- [38] G. R. You, G. J. Park, J. J. Lee, C. Kim, A colorimetric sensor for the sequential detection of  $\text{Cu}^{2+}$  and  $\text{CN}^-$  in fully aqueous media: practical performance of  $\text{Cu}^{2+}$ , *Dalton Trans.* 44 (2015) 9120–9129.
- [39] G. J. Park, I. H. Hwang, E. J. Song, H. Kim, C. Kim, A colorimetric and fluorescent sensor for sequential detection of copper ion and cyanide, *Tetrahedron* 70 (2014) 2822–2828.
- [40] Z. Liao, D. Wang, J.-Q. Zheng, H.-W. Tan, X.-J. Zheng, L.-P. Jin, A single chemosensor for bimetal Cu(II) and Zn(II) in aqueous medium, *RSC Adv.* 6 (2016) 33798–33803.
- [41] L. Tang, N. Wang, Q. Zhang, J. Guo, R. Nandhakumar, A new benzimidazole-based quinazoline derivative for highly selective sequential recognition of  $\text{Cu}^{2+}$  and  $\text{CN}^-$ , *Tetrahedron Lett.* 54 (2013) 536–540.
- [42] G. M. Credo, X. Su, K. Wu, O. H. Elibol, D. J. Liu, B. Reddy, Jr., T.-W. Tsai, B. R. Dorvel, J. S. Daniels, R. Bashir, M. Varma, Label-free electrical detection of pyrophosphate generated from DNA polymerase reactions on field-effect devices, *Analyst* 137 (2012) 1351–1362.
- [43] J. K. Heinonen, *Biological role of inorganic pyrophosphate*, Kluwer Academic Publishers, London, U.K., 2001.
- [44] B. M. Sefton, T. Hunter, *Protein Phosphorylation*; Academic Press: New York, 1998.
- [45] T. Pawson, J. D. Scott, Protein phosphorylation in signaling--50 years and counting, *Trends Biochem. Sci.* 30 (2005) 286–290.

- [46] J. R. Knowles, Enzyme-catalyzed phosphoryl transfer reactions, *Annu. Rev. Biochem.* 49 (1980) 877–919.
- [47] C. P. Mathews, K. E. van Hold, *Biochemistry*, The Benjamin/Cummings Publishing Co. Inc., Redwood City, CA, 1990.
- [48] K. T. Bush, S. H. Keller, S. K. Nigam, Genesis and reversal of the ischemic phenotype in epithelial cells, *J. Clin. Invest.* 106 (2000) 621–626.
- [49] P. MacMullan, G. McCarthy, Treatment and management of pseudogout: insights for the clinician, *Ther. Adv. Musculoskel. Dis.* 4 (2012) 121–131.
- [50] E. M. Farré, P. Geigenberger, L. Willmitzer, R. N. Trethewey, A Possible Role for Pyrophosphate in the Coordination of Cytosolic and Plastidial Carbon Metabolism within the Potato Tuber, *Plant Physiol.* 123 (2000) 681–688.
- [51] M. Hirose, J. Abe-Hashimoto, K. Ogura, H. Tahara, T. Ide and T. Yoshimura, A rapid, useful and quantitative method to measure telomerase activity by hybridization protection assay connected with a telomeric repeat amplification protocol, *J. Cancer Res. Clin. Oncol.* 123 (1997) 337–344.
- [52] M. Wang, D. Zhang, G. Zhang, Y. Tang, S. Wang, D. Zhu, Fluorescence Turn-On Detection of DNA and Label-Free Fluorescence Nuclease Assay Based on the Aggregation-Induced Emission of Silole, *Anal. Chem.* 80 (2008) 6443–6448.
- [53] R. Zhang, D. Tang, P. Lu, X. Yang, D. Liao, Y. Zhang, M. Zhang, C. Yu, V. W. Yam, Nucleic Acid-Induced Aggregation and Pyrene Excimer Formation, *Org. Lett.* 11 (2009) 4302–4305.
- [54] P. N. Basa, A. G. Sykes, Differential Sensing of Zn(II) and Cu(II) via Two Independent Mechanisms, *J. Org. Chem.* 77 (2012) 8428–8434.
- [55] J.-can Qin, Z.-Yin Yang, Fluorescent chemosensor for detection of Zn<sup>2+</sup> and Cu<sup>2+</sup> and its application in molecular logic gate, *J. Photochem. Photobiol. A: Chem.* 324 (2016) 152–158.
- [56] S. Anbu, A. Paul, G. J. Stasiuk, A. J. L. Pombeiro, Recent developments in molecular sensor designs for inorganic pyrophosphate detection and biological imaging, *Coord. Chem. Rev.* (2020) (accepted).
- [57] D. Buccella, J. A. Horowitz and S. J. Lippard, Understanding Zinc Quantification with Existing and Advanced Ditopic Fluorescent Zinpyr Sensors, *J. Am. Chem. Soc.* 133 (2011) 4101–4114.
- [58] B. A. Wong, S. Friedle and S. J. Lippard, Solution and Fluorescence Properties of Symmetric Dipicolylamine-Containing Dichlorofluorescein-Based Zn<sup>2+</sup> Sensors, *J. Am. Chem. Soc.* 131 (2009) 7142–7152.
- [59] M. A. Fox and M Chanon, *Photoinduced Electron Transfer*; Elsevier Science Publishers B.V.: New York, 1988.
- [60] M. Kumar, R. Kumar, V. Bhalla, P. R. Sharma, T. Kaur, Y. Qurishi, Thiocalix[4]arene based fluorescent probe for sensing and imaging of Fe<sup>3+</sup> ions, *Dalton Trans.* 41 (2012) 408–412.

- [61] T. Kowalczyk, Z. Lin, T.V. Voorhis, Fluorescence quenching by photoinduced electron transfer in the  $\text{Zn}^{2+}$  sensor Zinpyr-1: A computational investigation, *J. Phys. Chem. A* 114 (2010) 10427–10434.
- [62] A. W. Czarnik, *Fluorescent Chemosensors for Ion and Molecule Recognition*, American Chemical Society, Washington, DC, 1992.
- [63] R. W. Sinkeldam, N. J. Greco, Y. Tor, *Fluorescent Analogs of Biomolecular Building Blocks: Design, Properties, and Applications*, *Chem. Rev.* 110 (2010) 2579–2619.
- [64] X. B. Wang, X. Y. Ma, Z. Yang, Z. Zhang, J. H. Wen, Z. R. Geng, Z. L. Wang, AnNBD-armed tetraaza macrocyclic lysosomal-targeted fluorescent probe for imaging copper(II) ions, *Chem. Commun.* 49 (2013) 11263–11265.
- [65] H. M. Chawla, T. Gupta, Evaluation of a new calix[4] arene based molecular receptor for sensitive and selective recognition of  $\text{F}^-$  and  $\text{Cu}^{2+}$  ions, *J. Lumin.* 154 (2014) 89–94.
- [66] D. Ghosh, S. Rhodes, D. Winder, A. Atkinson, J. Gibson, W. Ming, C. Padgett, S. Landge and K. Aiken, Spectroscopic investigation of bis-appended 1,2,3-triazole probe for the detection of Cu(II) ion, *J. Mol. Str.* 1134 (2017) 638–648.
- [67] P. Ghorai, K. Pal, P. Karmakar, A. Saha, The development of two fluorescent chemosensors for the selective detection of  $\text{Zn}^{2+}$  and  $\text{Al}^{3+}$  ions in a quinoline platform by tuning the substituents in the receptor part: elucidation of the structures of the metal-bound chemosensors and biological studies, *Dalton Trans.* 49 (2020) 4758–4773.
- [68] N. A. Bumagina, E. V. Antina, A.Yu. Nikonova, M. B. Berezin, A. A. Ksenofontov and A. I. Vyugin, A New Sensitive and Selective Off-On Fluorescent  $\text{Zn}^{2+}$  Chemosensor Based on 3,3',5,5'-Tetraphenylsubstituted Dipyrromethene, *J. Fls.* 26 (2016) 1967–1974.
- [69] M. S. Kim, D. Yun, J. B. Chae, H. So, H. Lee, K.-T. Kim, M. Kim, M. H. Lim and C. Kim, A Novel Thiophene-Based Fluorescent Chemosensor for the Detection of  $\text{Zn}^{2+}$  and  $\text{CN}^-$ : Imaging Applications in Live Cells and Zebrafish, *Sensors* 19 (2019) 5458.
- [70] W. T. Tak, S. C. Yoon, Clinical Significance of Blood Level of Zinc and Copper in Chronic Renal Failure Patients, *Korean. J. Nephrol.* 20 (2001) 863–871.
- [71] W. Lin, D. Buccella, S. J. Lippard, Visualization of Peroxynitrite-Induced Changes of Labile  $\text{Zn}^{2+}$  in the Endoplasmic Reticulum with Benzoesorufin-Based Fluorescent Probes, *J. Am. Chem. Soc.* 135 (2013) 13512–13520.
- [72] S. K. Dey, M. A. Kobaisi, S. V. Bhosale, Functionalized Quinoxaline for Chromogenic and Fluorogenic Anion Sensing, *Chem. Open* 7 (2018) 934–952.
- [73] M. R. Maurya, A. Kumar, M. Ebel, D. Rehder, Synthesis, Characterization, Reactivity, and Catalytic Potential of Model Vanadium(IV, V) Complexes with Benzimidazole-Derived ONN Donor Ligands, *Inorg. Chem.* 45 (2006) 5924–5937.

- [74] R. Kaushik, A. Ghosh, A. Singh, P. Gupta, A. Mittal, D. A. Jose, Selective Detection of Cyanide in Water and Biological Samples by an Off-the-Shelf Compound, *ACS Sens.* 1 (2016) 1265–1271.
- [75] Z. Shojaeifard, B. Hemmateenejad, M. Shamsipur, Efficient On–Off Ratiometric Fluorescence Probe for Cyanide Ion Based on Perturbation of the Interaction between Gold Nanoclusters and a Copper(II)-Phthalocyanine Complex, *ACS Appl. Mater. Interfaces* 8 (2016) 15177–15186.
- [76] Y. L. Liu, X. Lv, Y. Zhao, J. Liu, Y. Q. Sun, P. Wang and W. Guo, A Cu(II)-based chemosensing ensemble bearing rhodamine B fluorophore for fluorescence turn-on detection of cyanide, *J. Mater. Chem.* 22 (2012) 1747–1750.
- [77] Y. S. Xie, Y. B. Ding, X. Li, C. Wang, J. P. Hill, K. Ariga, W. B. Zhang and W. H. Zhu, Selective, sensitive and reversible “turn-on” fluorescent cyanide probes based on 2,2'-dipyridylaminoanthracene–Cu<sup>2+</sup> ensembles, *Chem. Commun.* 48 (2012) 11513–11515.
- [78] R. K. Pathak, V. K. Hinge, A. Rai, D. Panda, C. P. Rao, Imino-phenolic-pyridyl conjugates of calix[4]arene (L1 and L2) as primary fluorescence switch-on sensors for Zn<sup>2+</sup> in solution and in HeLa cells and the recognition of pyrophosphate and ATP by [ZnL2]. *Inorg Chem.* 51 (2012) 4994–5005.
- [79] P. Raj, A. Singh, A. Singh, A. Singh, N. Garg, N. Kaur, N. Singh, Pyrophosphate Prompted Aggregation-Induced Emission: Chemosensor Studies, Cell Imaging, Cytotoxicity, and Hydrolysis of the Phosphoester Bond with Alkaline Phosphatase, *Eur. J. Inorg. Chem.* 5 (2019) 628–638.
- [80] B. K. Datta, S. Mukherjee, C. Kar, A. Ramesh, G. Das, Zn<sup>2+</sup> and pyrophosphate sensing: selective detection in physiological conditions and application in DNA-based estimation of bacterial cell numbers, *Anal. Chem.* 85 (2013) 8369–8375.
- [81] L. Tang, Z. Zheng, Z. Huang, K. Zhong, Y. Bian, R. Nandhakumar, Multi-analyte, ratiometric and relay recognition of a 2,5-diphenyl-1,3,4-oxadiazole-based fluorescent sensor through modulating ESIPT, *RSC Adv.* 5 (2015) 10505–10511.
- [82] J.-R. Lin, C.-J. Chu, P. Venkatesan, S.-P. Wu, Zinc(II) and pyrophosphate selective fluorescence probe and its application to living cell imaging, *Sensors and Actuators B* 207 (2015) 563–570.
- [83] Z. Hai, Y. Bao, Q. Miao, X. Yi and G. Liang, Pyridine-Biquinoline-Metal Complexes for Sensing Pyrophosphate and Hydrogen Sulfide in Aqueous Buffer and in Cells, *Anal. Chem.* 87 (2015) 2678–2684.
- [84] S. Anbu, S. Kamalraj, C. Jayabaskaran, P. S. Mukherjee, Naphthalene Carbohydrazone Based Dizinc(II) Chemosensor for a Pyrophosphate Ion and Its DNA Assessment Application in Polymerase Chain Reaction Products, *Inorg. Chem.* 52 (2013) 8294–8296.
- [85] S. Anbu, S. Kamalraj, A. Paul, C. Jayabaskaran, A. J. L. Pombeiro, The phenanthroimidazole-based dizinc(II) complex as a fluorescent probe for the pyrophosphate ion as generated in polymerase chain reactions and pyrosequencing, *Dalton Trans.* 44 (2015) 3930–3933.

- [86] R. G. Russell, S. Bisaz, A. Donath, D. B. Morgan, H. Fleisch, Inorganic pyrophosphate in plasma in normal persons and in patients with hypophosphatasia, osteogenesis imperfecta, and other disorders of bone, *J. Clin. Invest.* 50 (1971) 961–969.
- [87] G. Bülbül, A. Hayat, F. Mustafa, S. Andreescu, DNA assay based on Nanoceria as Fluorescence Quenchers (NanoCeracQ DNA assay), *Scientific Reports*, 8 (2018) 2426.
- [88] S. Bhaduri, N. Ranjan, D. P. Arya, An overview of recent advances in duplex DNA recognition by small molecules, *Beilstein J. Org. Chem.* 14 (2018) 1051–1086.
- [89] J. Liu, Z. Cao, Y. Lu, Functional Nucleic Acid Sensors, *Chem. Rev.* 109 (2009) 1948–1998.
- [90] A. Pal, Y. Levy, Structure, stability and specificity of the binding of ssDNA and ssRNA with proteins, *PLoS Comput Biol.* 15 (2019) e1006768.
- [91] D. Jose, K. Datta, N. P. Johnson, P. H. von Hippel, Spectroscopic studies of position-specific DNA “breathing” fluctuations at replication forks and primer-template junctions, *PNAS*, 106 (2009) 4231–4236.
- [92] W. M. Lau, M. Doucet, R. Stadel, D. Huang, K. L. Weber, S. L. Kominsky, Enpp1: A Potential Facilitator of Breast Cancer Bone Metastasis, *PLoS One* 8(7) (2013) e66752.
- [93] M. Hirose, J. Abe-Hashimoto, K. Ogura, H. Tahara, T. Ide, T. Yoshimura, A rapid, useful and quantitative method to measure telomerase activity by hybridization protection assay connected with a telomeric repeat amplification protocol, *J. Cancer Res. Clin. Oncol.* 123 (1997) 337–344.
- [94] G. Theiler, F. Quehenberger, F. Rainer, M. Neubauer, M. Stettin, C. Robier, The detection of calcium pyrophosphate crystals in the synovial fluid of patients with rheumatoid arthritis using the cytospin technique: prevalence and clinical correlation, *Rheumatol. Int.* 34 (2014) 137–139.
- [95] J. F. Fahrman, K. Kim, B. C. DeFelice, S. L. Taylor, D. R. Gandara, K. Y. Yoneda, D. T. Cooke, O. Fiehn, K. Kelly, S. Miyamoto, Investigation of Metabolomic Blood Biomarkers for Detection of Adenocarcinoma Lung Cancer, *Cancer Epidemiol. Biomarkers Prev.* 24 (2015) 1716–1723.
- [96] J. K. Heinonen, Biological role of inorganic pyrophosphate, Kluwer Academic Publishers, London, U.K., 2001.
- [97] C. T. Harrington, E. I. Lin, M. T. Olson, J. R. Eshleman, *Arch. Pathol. Lab. Med.*, 137 (2013) 1296–1303.
- [98] E. Ekrami, M. Pouresmaeli, F. Barati, S. Asghari, F. R. Ziarani, P. Shariati, M. Mamoudifard, Potential Diagnostic Systems for Coronavirus Detection: a Critical Review, *Biol. Proced. Online* 22 (2020) 21.
- [99] C. P. Mathews, K. E. van Hold, *Biochemistry*; The Benjamin/Cummings Publishing Company, Inc.: Redwood City, CA, 1990.

- [100] M. Ronaghi, S. Karamohamed, B. Pettersson, M. Uhlen, P. Nyren, Real-time DNA sequencing using detection of pyrophosphate release, *Anal. Biochem.* 242 (1996) 84–89.
- [101] W. Zhu, X. Huang, Z. Guo, X. Wu, H. Yu, H. Tian, A novel NIR fluorescent turn-on sensor for the detection of pyrophosphate anion in complete water system, *Chem. Commun.* 48 (2012) 1784–1786.
- [102] S. Dey, P. K. Sukul, Selective Detection of Pyrophosphate Anions in Aqueous Medium Using Aggregation of Perylene Diimide as a Fluorescent Probe, *ACS Omega* 4 (2019) 16191–16200.
- [103] Q. Meng, Y. Wang, H. Feng, F. Zhou, B. Zhou, C. Wang, R. Zhang, Z. Zhang, A novel glucosamine-linked fluorescent chemosensor for the detection of pyrophosphate in an aqueous medium and live cells, *New J. Chem.* 42 (2018) 2675–2681.
- [104] S. Anbu, R. Ravishankaran, M. F. C. G. da Silva, A. A. Karande, A. J. L. Pombeiro, Differentially Selective Chemosensor with Fluorescence Off–On Responses on  $\text{Cu}^{2+}$  and  $\text{Zn}^{2+}$  Ions in Aqueous Media and Applications in Pyrophosphate Sensing, Live Cell Imaging, and Cytotoxicity, *Inorg. Chem.* 53 (2014) 6655–6664.
- [105] J. Wang, B. Liu, X. Liu, M.J. Panzner, C. Wesdemiotis, Y. Pang, A binuclear Zn(ii)–Zn(ii) complex from a 2-hydroxybenzohydrazide-derived Schiff base for selective detection of pyrophosphate, *Dalton Trans.* 43 (2014) 14142–14146.
- [106] A. Gogoi, S. Mukherjee, A. Ramesh, G. Das, Nanomolar Zn(ii) sensing and subsequent PPI detection in physiological medium and live cells with a benzothiazole functionalized chemosensor, *RSC Adv.* 5 (2015) 63634–63640.
- [107] C. Chang, F. Wang, T. Wei, X. Chen, Benzothiazole-Based Fluorescent Sensor for Ratiometric Detection of Zn(II) Ions and Secondary Sensing PPI and Its Applications for Biological Imaging and PPase Catalysis Assays, *Ind. Eng. Chem. Res.* 56 (2017) 8797–8805.
- [108] J. Wang, X. Liu, Y. Pang, A Benzothiazole-Based Sensor for Pyrophosphate (PPI) and ATP: Mechanistic Insight for Anion-Induced ESIPT Turn-On, *J. Mater. Chem. B* 2 (2014) 6634–6638.
- [109]. X. Chen, S.-W. Nam, G.-H. Kim, N. Song, Y. Jeong, I. Shin, S.K. Kim, J. Kim, S. Park, J. Yoon, A Near-Infrared Fluorescent Sensor for Detection of Cyanide in Aqueous Solution and Its Application for Bioimaging. *Chem. Commun.* 46 (2010) 8953–8955.
- [110] L. Qin, L. Hou, J. Feng, J. Chao, Y. Wang, W. J. Jin, A novel chemosensor with visible light excitability for sensing  $\text{CN}^-$  in aqueous medium and living cells via a  $\text{Cu}^{2+}$  displacement approach, *Anal. Methods*, 9 (2017) 259–266.
- [111] F.-Y. Wu, F.-Y. Xie, Y.-M. Wu and J.-I. Hong, Interaction of a New Fluorescent Probe with DNA and its Use in Determination of DNA, *J. Fluores.* 18 (2008) 175–181.

[112] W. A. Durai and A. Ramu, Hydrazone Based Dual - Responsive Colorimetric and Ratiometric Chemosensor for the Detection of  $\text{Cu}^{2+}/\text{F}^-$  Ions: DNA Tracking, Practical Performance in Environmental Samples and Tooth Paste, *J. Fluores.* 30 (2020) 275–289.

## Authors Biographies

1. **Sellamuthu Anbu** received the PhD degree in Inorganic Chemistry in 2010 from University of Madras, India. After spending a semester working as a lecturer in National Institute of Technology-Calicut, India, he joined the supramolecular chemistry research group of Prof. Partha Sarathi Mukherjee at the Indian Institute of Science in 2011 as a UGC-Kothari postdoctoral fellow. In 2012, he subsequently joined as an FCT-Postdoctoral fellow in the group of Prof. Armando J. L. Pombeiro at the Instituto Superior Tecnico, Portugal, and involved in the development of fluorescent sensors. In 2015, he was awarded the Marie Sklodowska-Curie Individual Fellowship by European Commission to continue his pioneering research in bioinorganic chemistry with the group of Dr Anna Peacock, University of Birmingham, UK. Since 2018, he has been a visiting researcher in the group of Dr Graeme J. Stasiuk at the University of Hull, UK, working on the development of anion responsive magnetic resonance contrast agents with the support of the Royal Society of Chemistry research grant fund award. He published 29 papers in high quality peer-reviewed international journals (1198–google citations, 'h' index–20) and contributed to more than 40-national/international conferences.
2. **Anup Paul** was born in Tura, Meghalaya, India. He obtained his PhD in 2012 from North-Eastern Hill University (NEHU), Shillong, India, under Prof. T. S. BasuBaul. He joined at Instituto Superior Tecnico, Lisbon, Portugal as an FCT postdoctoral fellow under Prof. Armando J. L. Pombeiro and is currently working as an integrated researcher in the same institution. His current research interests focus on bioinorganic chemistry and the construction and application of metal-organic frameworks in catalysis and sensing.
3. **Kalpana Surendranath (KS)** is a Senior Lecturer in Life Sciences and the leader of Genome Engineering Lab at the University of Westminster. KS joined as a full-time member of Faculty of Biomedical Sciences at the University of Westminster in Oct 2017 where her time is divided between teaching and research. She introduced CRISPR genome engineering technology to both teachings and in research at the University in 2017 and ever since her laboratory has won several awards: Royal Society's top project award at the house of commons, UK parliament, 3 continuous years of the 125 fund, Genetics Society summer grant among others. Dr Kalpana also runs the Institute of Biomedical Sciences (IBMS) accredited short course in human genome engineering. KS has received notable awards and grants, throughout her career, recent ones include Children with Cancer UK (2020) Quintin Hogg Trust (2020), Genetics Society (2019), Royal Society top project award (2018), 125 funds (2018, 2019 and 2020). She conceived the "gene editors of the future" student training and development programme and awarded by Quintin Hogg Trust this year. She also received the highest honour of the University "the Vice-Chancellor's WestminsterSTAR award", Women of Westminster award, the individual award for teaching excellence and Westminster Champion award for an educational experience in the years 2018-2020. KS is a London STEM ambassador, Aurora AdvanceHE UK women leadership in a higher education role model.

4. **Nadeen Shaikh Solaiman** completed undergraduate studies in American University of Sharjah and joined master's in biomedical sciences at the University of Westminster. Her interest in Genome engineering led to doctoral studies on the exploring the novel roles of RNA binding proteins in maintenance of genome stability. She is also a part-time visiting lecturer at the University of Westminster and has experience working as a medical laboratory scientist in molecular pathology department of Health services Laboratories, London United Kingdom.
5. **Armando J. L. Pombeiro** is Full Professor Jubilado at Instituto Superior Técnico, Universidade de Lisboa, Fellow of the European Academy of Sciences and Full Member of the Academy of Sciences of Lisbon. His research group investigates the activation of small molecules with industrial, environmental or biological significance, including metal-mediated synthesis and catalysis, crystal engineering of coordination compounds, design and self-assembly of polynuclear and supramolecular structures, non-covalent interactions, molecular electrochemistry and theoretical studies. He authored one book, edited 6 books, (co-)authored ca. 895 research publications and ca. 40 patents, and presented more 115 plenary and keynote lectures at international conferences. His work has received ca. 23,500 citations, h-index = 68 (Web of Science). Among his honours, he was awarded the Franco-Portugais Prix of the French Chemical Society, the Madinabeitia-Lourenço Prize from the Spanish Royal Chemical Society, the Vanadis Prize, the Prizes of the Portuguese Chemical and Electrochemical Societies, and the Scientific Prizes of the Technical University of Lisbon and of the University of Lisbon.

## Declaration of interests

The authors declare that they have no known competing financial interests or personal relationships that could have appeared to influence the work reported in this paper.

Dr. Sellamuthu Anbu

Dr. Anup Paul

Dr. Kalpana Surendranath

Ms. Nadeen Shaikh Solaiman

Prof. Armando J. L. Pombeiro



Click here to access/download

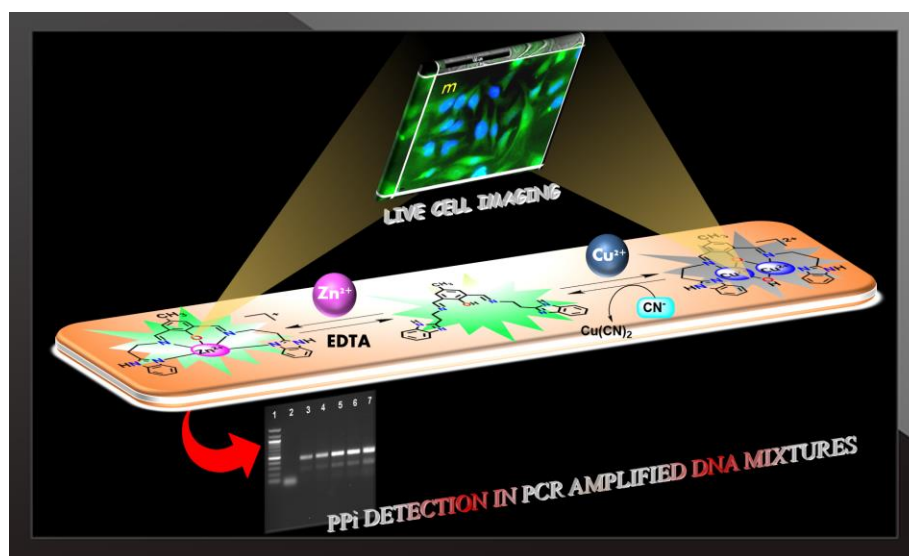
**Supplementary Material**

S&A-Supplementary\_Information\_SA\_1.doc



**A benzimidazole-based new fluorogenic differential/sequential chemosensor for  $\text{Cu}^{2+}$ ,  $\text{Zn}^{2+}$ ,  $\text{CN}^-$ ,  $\text{P}_2\text{O}_7^{4-}$ , DNA, its live-cell imaging and pyrosequencing applications**

Sellamuthu Anbu,<sup>a,b\*</sup> Anup Paul,<sup>a</sup> Kalpana Surendranath,<sup>c</sup> Nadeen Sheikh Solaiman,<sup>c</sup>  
Armando J. L. Pombeiro<sup>a</sup>



A benzimidazole-based chemosensor (**DFB**) for  $\text{Cu}^{2+}$  and  $\text{Zn}^{2+}$  was developed, and its sequential anions ( $\text{CN}^-$  and  $\text{P}_2\text{O}_7^{4-}$ ) and DNA sensing capability and its live-cell imaging, as well as its  $\text{PPi}$  detection in PCR-amplified DNA products, has been demonstrated.